Journal of Electronics, Electromedical Engineering, and Medical Informatics
Homepage: jeeemi.org; Vol. 9, No. 1, January 2027, pp: 54-76 e-ISSN: 2656-8632
RESEARCH ARTICLE OPEN ACCESS

# Comparative Cyclic Mechanical Response of Commercial SACH Prosthetic Feet under ISO 10328-Based Fatigue Loading

**Mahfud Saifudin, Nur Rachmat*, Sisybania, and Anissa Eka Septiani**
**Department of Prosthetic Orthotic, Poltekkes Kemenkes Surakarta, Surakarta, Indonesia**
**Corresponding author**: Nur Rachmat (e-mail: nurrachmat@gmail.com), **Author(s) Email**: Mahfud Saifudin (e-mail: saepsyaifudin@gmail.com), Sisybania (e-mail: sisybania@gmail.com), Anissa Eka Septiani (e-mail: sanissaeka@gmail.com)

## Abstract

**Background**: The Solid Ankle Cushion Heel (SACH) foot remains widely prescribed in lower-limb prosthetic rehabilitation, particularly in low- and middle-income countries, because of its simple construction, low maintenance demand, and affordability. However, commercially supplied SACH feet that appear externally similar may respond differently to repetitive loading, and procurement decisions are frequently based on internal inventory labels rather than independent mechanical evidence. Previous studies have mainly characterized prototype designs or single reference feet under static or quasi-static loading, so comparative cyclic evidence for finished commercial SACH feet remains scarce.

**Aims**: This exploratory study aimed to compare the early observable cyclic mechanical response of two commercial SACH foot groups and to establish a reproducible screening framework for finished commercial components.

**Methods**: Six new right-sided SACH feet were tested: three Group B specimens (sizes 23R, 24R, and 25R) and three size-matched Group A specimens. A pneumatic fatigue tester applied alternating heel and forefoot loading following the principles of ISO 10328:2016, Section 17.2.5, with a target range of 50–1,330 N at 1 Hz; the recorded maximum load was 1,460 N for all specimens, representing a 9.8% overshoot. The predefined endpoint was the first visible microdeformation, and specimens without an event were treated as right-censored observations.

**Results**: All three Group B specimens (3/3, 100%) developed visible dorsal microdeformation at 10,000 cycles, whereas none of the Group A specimens (0/3, 0%) showed a comparable abnormality through 100,000 cycles. One Group B specimen was inadvertently continued to 150,000 cycles after its endpoint because of a protocol communication error. No specimen developed cracking, delamination, permanent deformation, loss of fit, or structural failure.

**Conclusion**: The scientific contribution of this study is a comparative, endpoint-driven evaluation of finished commercial SACH feet, rather than prototype development, under identical cyclic loading. The findings indicate a consistent difference in early cyclic response under the applied protocol. However, the small sample, visual endpoint assessment, load overshoot, unequal test exposure, and absence of testing to failure preclude conclusions regarding comparative fatigue life or ISO conformity.

**Keywords**: SACH foot; prosthetic foot; fatigue testing; cyclic loading; mechanical durability; rehabilitation engineering.

## I. Introduction

Lower-limb prosthetic feet form the distal mechanical interface between the user and the ground, thereby influencing load transfer, shock attenuation, progression, stability, and the overall reliability of the prosthetic system. Although advanced energy-storing and energy-returning feet have expanded substantially, the Solid Ankle Cushion Heel (SACH) foot remains an important component of routine prosthetic care because of its simple, non-articulated architecture, low maintenance requirements, relatively low cost, and wide availability in resource-constrained settings [1], [2], [3], [4], [5], [6]. For health systems in low- and middle-income countries, these characteristics are not merely economic considerations; they directly affect continuity of mobility when sophisticated replacement

Manuscript Received 16 September 2026; Accepted: 10 November 2026; Published online: 20 November 2026
**Digital Object Identifier (DOI):** https://doi.org/10.35882/jeeemi.v9i1.1921
**Copyright** © 2026 by the authors. Published by Jurusan Teknik Elektromedik, Politeknik Kesehatan Kemenkes Surabaya Indonesia. This work is an open-access article and licensed under a Creative Commons Attribution-ShareAlike 4.0 International License (CC BY-SA 4.0).

parts, specialized maintenance, or high-cost dynamic-response components are not consistently accessible [2], [4], [6].

The mechanical behavior of a SACH foot is determined by the interaction of its keel, compliant heel region, external foot shell, and attachment structure. During walking, these elements are repeatedly loaded during initial contact, mid-stance, and terminal stance. Even when a component performs adequately under a single static load, repetitive cyclic loading may initiate local deformation, progressive material damage, delamination, stiffness changes, or eventual structural failure. Consequently, fatigue behavior is a critical engineering dimension of prosthetic-foot quality that cannot be inferred reliably from appearance, retail price, or commercial labeling alone [7], [8], [9], [10], [11], [12], [13]. Recent prosthetic-foot research has focused on material substitution, numerical optimization, and experimental validation. Polymer and composite keel designs have been investigated to improve structural consistency while retaining manufacturability and affordability [1], [9], [12], [13], [14], [15], [16], [17]. Finite element analyses have demonstrated that keel geometry, elastic modulus, stress concentration, and boundary conditions substantially influence total deformation and local mechanical response [3], [9], [15], [17], [18], [19], [20], [21], [28]. Clinical and biomechanical studies further show that prosthetic-foot stiffness and structural behavior can alter foot-ankle mechanics and user perception, indicating that mechanical design variables have consequences beyond laboratory performance [22], [23].

Despite these advances, three limitations of the current state of the art remain relevant to routine prosthetic services. First, most finite element investigations rely on static or quasi-static boundary conditions that represent discrete gait instants, and their experimental validation is commonly restricted to static loading, for example up to 1,176.78 N for a polymer-keel SACH foot [1] or static ISO 10328:2016 loading of a composite SACH foot with a mean numerical error below 15.22% [13]; such studies do not describe how finished feet respond to accumulated loading cycles. Second, fatigue-testing studies have mainly addressed prototype feet or a single reference product. Abdalwahhab et al. reported fatigue lives of 510,382 cycles for a new flexible-keel foot and 473,241 cycles for a SACH foot [25], and Sasaki et al. completed two million cycles at 1.28 kN for a modified natural-rubber SACH foot [42]. Third, large-scale ISO 10328 testing of 21 foot models used in low-income countries showed that none passed the strictest protocol and that all but one failed the initial static proof test because of permanent forefoot deformation [40], whereas heavy-duty commercial feet passed P5 cyclic testing but still showed significant changes in stiffness and creep after cycling [41]. These findings indicate that durability can differ substantially among commercially available feet, yet comparative cyclic evidence for finished SACH feet supplied through the same procurement channel remains scarce. A recent JEEEMI study by Nugroho et al. combined finite element analysis and experimental validation to evaluate a polymer-keel SACH foot and showed that structural material and keel configuration can meaningfully modify deformation and load distribution under ISO 10328-based loading [1]. That study addressed design development and quasi-static validation. A different but related problem exists in routine prosthetic procurement: commercially supplied SACH feet may be distributed under internal inventory categories despite limited independent evidence describing whether the products respond similarly to repetitive loading. This gap is especially relevant when components are selected for cost-sensitive services

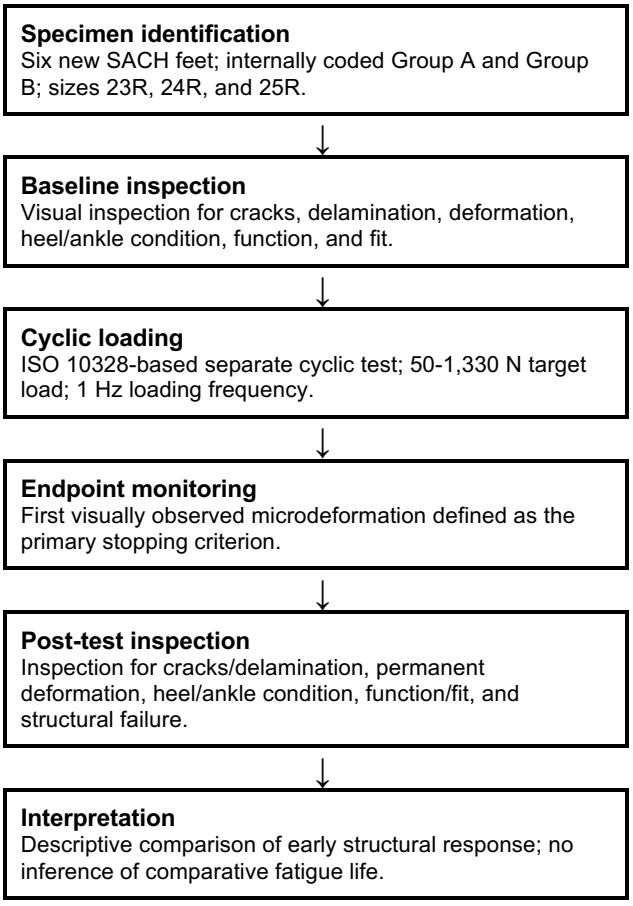



**Fig. 1. Experimental workflow for comparative cyclic fatigue evaluation of commercial SACH prosthetic feet, illustrating specimen preparation, ISO 10328-based loading, microdeformation detection, structural inspection, and descriptive outcome analysis.**

Manuscript Received 16 September 2026; Accepted: 10 November 2026; Published online: 20 November 2026
**Digital Object Identifier (DOI):** https://doi.org/10.35882/jeeemi.v9i1.1921
**Copyright** © 2026 by the authors. Published by Jurusan Teknik Elektromedik, Politeknik Kesehatan Kemenkes Surabaya Indonesia. This work is an open-access article and licensed under a Creative Commons Attribution-ShareAlike 4.0 International License (CC BY-SA 4.0).

and when manufacturer-specific mechanical data are unavailable or insufficiently detailed. In the present setting, two commercially supplied SACH foot groups were managed using internal inventory labels, here anonymized as Group A and Group B. These labels were not manufacturer-certified quality grades and were not intended to represent an international engineering classification. Prior to this study, no internal laboratory evidence was available to compare the cyclic mechanical response of the two product groups under the same testing framework. The novelty of the study therefore lies in comparative quality-assurance testing of finished commercial SACH feet rather than in the development of a new prosthetic-foot design.

The research gap can therefore be stated explicitly. Existing finite element and fatigue-testing studies have primarily characterized new designs, prototype materials, or single reference feet, whereas no comparable evidence was available for size-matched, finished commercial SACH feet distributed under internal inventory categories and evaluated under the same cyclic-loading framework with a predefined early structural endpoint. To address this gap, the present study adopted an endpoint-driven experimental approach in which commercial feet were subjected to ISO 10328-based alternating heel and forefoot cyclic loading, inspected for the first visible microdeformation, and analyzed descriptively with right-censoring for specimens that did not reach the endpoint. The objective was to compare the early observable structural response of Group A and Group B SACH feet during ISO 10328-based cyclic fatigue loading. The primary endpoint was first visible microdeformation, supplemented by observation of cracking or delamination, permanent deformation, functional or fitting abnormality, and structural failure. The study was intentionally interpreted as an exploratory mechanical evaluation because of the small number of specimens and the absence of standardized testing to complete failure.

The scientific contributions of this study are threefold. First, it provides specimen-level comparative data on the early cyclic response of six size-matched, finished commercial SACH feet tested under identical loading settings, with transparent reporting of the 9.8% load overshoot and one protocol deviation. Second, it formulates an explicit mathematical and operational framework that links the cyclic-loading parameters, load deviation, cycle exposure, censored endpoints, and measurement uncertainty to the available laboratory records. Third, it proposes a staged and reproducible quality-assurance pathway that distinguishes visually observed microdeformation from quantitatively established permanent deformation and structural failure, which can be applied to the incoming inspection of prosthetic feet in cost-sensitive services.

## II. Method

### A. Study Design and Research Setting

A comparative laboratory-based mechanical experiment was conducted to characterize the cyclic response of two commercially supplied SACH prosthetic-foot groups. Testing was performed on 29 April 2026 at the Mechatronics Laboratory, Universitas Islam Indonesia, Yogyakarta, Indonesia. The laboratory report was prepared by the test operator and independently reviewed and approved within the laboratory quality process. No human participants, biological samples, or patient-identifiable data were involved. The protocol used the principles of ISO 10328:2016, specifically Section 17.2.5 for separate cyclic testing of ankle-foot devices and foot units [24]. The study was not designed to certify the products for regulatory conformity. Instead, the standard was used as a structured engineering framework to create repeatable cyclic loading and predefined observation criteria. The overall experimental workflow, from specimen identification and baseline inspection to cyclic loading, endpoint monitoring, post-test inspection, and interpretation, is illustrated in Fig. 1.

**Table 1. Identification, commercial group classification, nominal size, laterality, and baseline structural condition of the six SACH prosthetic-foot specimens evaluated under cyclic fatigue loading.**

| Specimen | Group | Size/side | Baseline |
|---|---|---|---|
| SACH-01 | B | 23R | New, intact |
| SACH-02 | B | 24R | New, intact |
| SACH-03 | B | 25R | New, intact |
| SACH-04 | A | 23R | New, intact |
| SACH-05 | A | 24R | New, intact |
| SACH-06 | A | 25R | New, intact |

### B. Specimens and Group Classification

Six new right-sided SACH feet were evaluated. Three specimens were assigned to Group B (SACH-01 to SACH-03) and three to Group A (SACH-04 to SACH-06). Each group included nominal foot sizes 23R, 24R, and 25R. All specimens were unused before testing and were visually inspected for pre-existing cracks, deformation, modification, or attachment abnormalities.

The Group A and Group B labels were internal inventory codes used by the supplying organization and were not manufacturer names, formal quality grades, or certified material classifications. The commercial identity was therefore anonymized in the

Manuscript Received 16 September 2026; Accepted: 10 November 2026; Published online: 20 November 2026
**Digital Object Identifier (DOI):** https://doi.org/10.35882/jeeemi.v9i1.1921
**Copyright** © 2026 by the authors. Published by Jurusan Teknik Elektromedik, Politeknik Kesehatan Kemenkes Surabaya Indonesia. This work is an open-access article and licensed under a Creative Commons Attribution-ShareAlike 4.0 International License (CC BY-SA 4.0).

manuscript to avoid implying an unsupported hierarchy of manufacturing quality. Because detailed manufacturer material specifications were unavailable, interpretation was restricted to the observed behavior of the tested product groups. The specimen identification, group allocation, nominal size, side, and baseline condition are summarized in Table 1.

### C. Fatigue Test Apparatus and Loading Procedure

The fatigue-test system used pneumatic actuation to apply repeated mechanical loading to a SACH foot mounted on a prosthetic pylon. The apparatus was configured to reproduce repeated loading of the prosthetic foot using two loading regions that approximate heel and forefoot contact during gait. This type of controlled cyclic testing is relevant because repeated gait loading can reveal structural changes not apparent during single-load or purely static evaluation [7], [10], [13], [25], [26]. The test rig comprised a compressed-air supply, a pressure regulator and filter used to set the loading level, solenoid valves that alternately pressurized two pneumatic cylinders, a heel loading platform and a forefoot loading platform, a specimen fixture consisting of a pylon and pyramid adapter, a force transducer, and a controller with a cycle counter and monitor. A comparable pneumatic heel-and-forefoot fatigue tester has previously been used to evaluate SACH and flexible-keel feet [25]. For the separate cyclic test of ankle-foot devices and foot units, ISO 10328:2016 specifies a pulsating test force applied alternately to the heel and forefoot, with loading-platform inclinations of 15° for the heel and 20° for the forefoot; at test loading level P5, the force pulsates between 50 N and 1,330 N for a prescribed 2,000,000 cycles [24], [40], [41]. The present protocol adopted the P5 force range and a frequency of 1 Hz but was terminated at the predefined visual endpoint rather than at the prescribed cycle count. The following laboratory details were not available in the research dataset and are therefore reported as missing information rather than estimated: cylinder bore and stroke, regulator pressure, actual platform angles, fixture alignment offsets, load-cell model and accuracy class, calibration date and certificate, and force-sampling rate.

The target cyclic loading range was 50 N to 1,330 N at a frequency of 1 Hz. During testing, the laboratory acquisition record documented an actual maximum load of 1,460 N for all six specimens. Thus, the actual recorded peak exceeded the target maximum by approximately 9.8%. Because the same recorded maximum was documented for all specimens, internal comparison between groups was maintained; however, this load overshoot was treated as a methodological deviation and is considered in the limitations.

The implications of this deviation for experimental validity are threefold. First, because the identical recorded maximum of 1,460 N was documented for every specimen, the deviation did not bias the between-group comparison. Second, the recorded peak exceeded the intended P5 cyclic level by 130 N but remained 780 N (34.8%) below the 2,240 N static proof load used in ISO 10328 foot testing [40]; the overshoot therefore represents a more severe cyclic condition rather than a static overload beyond the proof level. Third, according to stress–life relations (Section II.G), a higher load amplitude is expected to reduce the number of cycles to a given damage state [45], [49]. Consequently, the cycle counts reported here should be regarded as conservative, potentially earlier, estimates relative to testing at exactly 1,330 N, and conformity with the ISO 10328 force tolerance cannot be claimed.

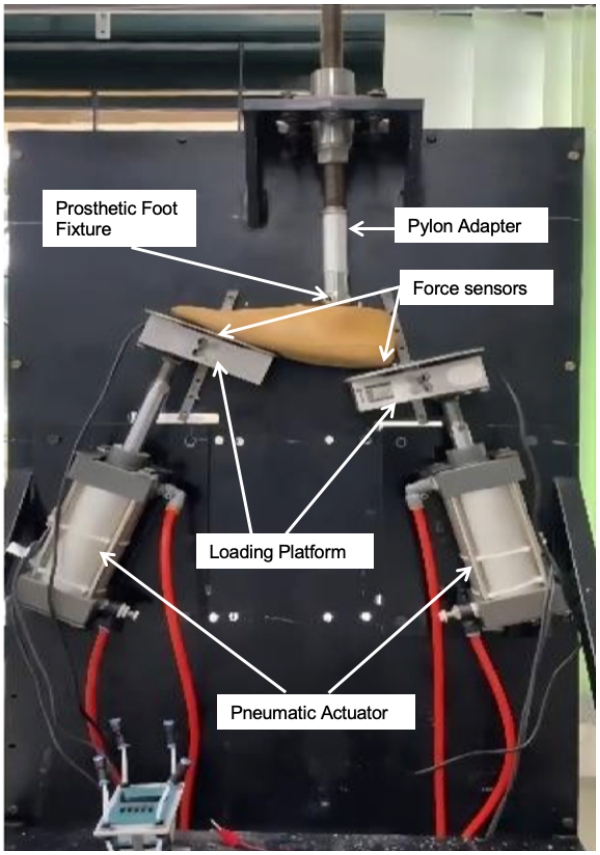



**Fig. 2. Experimental pneumatic fatigue-testing apparatus showing the SACH prosthetic-foot mounting configuration, heel and forefoot loading mechanisms, pneumatic actuators, and force measurement system used during cyclic testing.**

The predefined stop criterion was the first occurrence of visible microdeformation. There was no fixed target cycle count in the laboratory request. Specimens were monitored during testing and underwent pre-test and post-test visual inspection of the overall shell, heel material, ankle region, cracking or delamination, permanent deformation,

Manuscript Received 16 September 2026; Accepted: 10 November 2026; Published online: 20 November 2026
**Digital Object Identifier (DOI):** https://doi.org/10.35882/jeeemi.v9i1.1921
**Copyright** © 2026 by the authors. Published by Jurusan Teknik Elektromedik, Politeknik Kesehatan Kemenkes Surabaya Indonesia. This work is an open-access article and licensed under a Creative Commons Attribution-ShareAlike 4.0 International License (CC BY-SA 4.0).

microdeformation, and functional fit. The pneumatic fatigue-test apparatus and specimen mounting configuration used for cyclic loading are shown in Fig. 2. The target loading conditions, recorded maximum load, loading frequency, and predefined stopping criterion are summarized in Table 2.

The engineering configuration of the test system, including the pneumatic actuation chain, loading mechanism, prosthetic-foot fixture, force measurement, monitoring procedure, and endpoint-detection logic, is presented as a block diagram in Fig. 3. The step-by-step testing algorithm, comprising specimen preparation, cyclic loading, inspection, stopping decisions, and data recording, is given in Algorithm 1. Parameters that were measured and recorded by the laboratory (target minimum and maximum loads, recorded maximum load, frequency, cycle counts, pre-test and post-test condition, and photographs) are distinguished from parameters that were unavailable in the laboratory records (continuous force–time traces, displacement, strain, calibration certificates, and fixture angles).

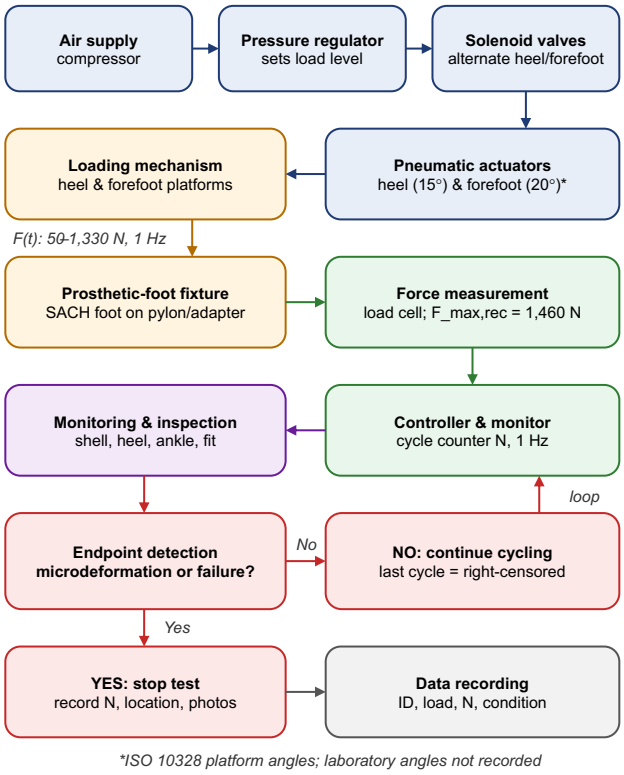



**Fig. 3. Functional block diagram of the pneumatic cyclic fatigue-testing system, illustrating the actuation mechanism, alternating heel–forefoot loading, force measurement, cycle monitoring, structural inspection, and endpoint-based stopping procedure. Platform inclinations of 15° (heel) and 20° (forefoot) are nominal ISO 10328 values; the platform angles actually set during the experiments were not recorded.**

### D. Outcome Definition and Protocol Deviation

The primary mechanical endpoint was the cycle count at which visible microdeformation was first detected. Microdeformation was operationally defined as an observable localized change in shape that did not constitute cracking, delamination, permanent gross deformation, loss of attachment, loss of fit, or complete structural failure. Secondary outcomes were the presence or absence of crack or delamination, permanent deformation, abnormality of the heel or ankle region, functional or fit impairment, and structural failure.

Microdeformation was identified by direct visual inspection performed by the laboratory test operator. The laboratory records do not document magnification, lighting conditions, a calibrated scale in the photographs, blinding of the operator to group allocation, or confirmation by a second independent observer; therefore, observer subjectivity may have influenced both the detection threshold and the cycle at which an event was recognized. Because inspection was linked to cycle checkpoints, the true onset of microdeformation in Group B lies within the interval preceding the first checkpoint at which it was recorded, that is, $0 < N_{onset} \leq 10{,}000$ cycles. In this manuscript, microdeformation therefore denotes a visually observed localized change in shape and is explicitly distinguished from quantitatively established permanent deformation, which requires displacement or surface-profile measurement after unloading [40], [41]. For SACH-01, visible microdeformation was first documented at 10,000 cycles, but the test inadvertently continued to 150,000 cycles because of a communication error between the research team and laboratory personnel. This was treated as a protocol deviation. For comparative analysis, the valid endpoint for SACH-01 remained the first observed microdeformation at 10,000 cycles. The additional cycles were reported transparently but were not interpreted as evidence of superior fatigue resistance or extended fatigue life.

### E. Data Analysis

Because the sample comprised only three specimens per group and the study was not powered for statistical inference, the analysis was descriptive. Results were summarized at the individual-specimen level and by product group. The principal comparison was whether visible microdeformation occurred by 10,000 cycles and whether specimens remained free of the predefined structural abnormalities through the observed test period. Event proportions with 95% Wilson score intervals and Kaplan–Meier estimates that treat specimens without an event as right-censored observations were calculated descriptively using Eqs.

Manuscript Received 16 September 2026; Accepted: 10 November 2026; Published online: 20 November 2026
**Digital Object Identifier (DOI):** https://doi.org/10.35882/jeeemi.v9i1.1921
**Copyright** © 2026 by the authors. Published by Jurusan Teknik Elektromedik, Politeknik Kesehatan Kemenkes Surabaya Indonesia. This work is an open-access article and licensed under a Creative Commons Attribution-ShareAlike 4.0 International License (CC BY-SA 4.0).

**Algorithm 1: Step-by-step cyclic fatigue-testing and endpoint-detection procedure for commercial SACH prosthetic feet, including specimen preparation, ISO 10328-based alternating heel–forefoot loading, cycle counting, periodic structural inspection, identification of microdeformation or failure, right-censoring, and post-test documentation.**

**Input:** Specimens SACH-01 to SACH-06; $F_{min}$ = 50 N; $F_{max}$ = 1,330 N; $f$ = 1 Hz; endpoint = first visible microdeformation
**Output:** Cycle count at endpoint (event) or last observed cycle (right-censored); post-test inspection record; photographs
**Procedure** *FatigueTest*(*S*):
**for each** specimen $S_i$ **do**
  Record identity, group code, size, side, and baseline condition (Table 1); photograph $S_i$
  Inspect shell, heel, ankle region, connector, and fit
  **if** a pre-existing defect is found **then**
    Exclude $S_i$; **continue**
  **end**
  Mount $S_i$ on the pylon/adapter fixture; align the heel and forefoot with the loading platforms
  Set the regulator pressure for the target load; start alternating heel–forefoot loading at $f$ = 1 Hz; $N \leftarrow 0$
  **while** no endpoint is detected **do**
    Apply load cycles; update $N$ from the cycle counter; record the measured peak force
    **if** $N$ reaches an inspection checkpoint (first at $N$ = 10,000) **then**
      Pause and inspect the dorsal shell, heel, ankle region, and attachment
      **if** crack, delamination, loss of fit, or structural failure is observed **then**
        Record $N_{fail}$; **break**
      **else if** visible microdeformation is observed **then**
        Record $N_{event}$, location, and photographs; **break**
      **else if** the observation limit is reached without an event **then**
        Record $N_{last}$ as right-censored; **break**
      **end**
    **end**
  **end**
  Stop loading; unload; perform post-test inspection (Table 5 items); photograph and archive the record
**end**
**Return** endpoint records ($N_{fail}$, $N_{event}$, or $N_{last}$) for all specimens

(26)–(28) in Section II.G. No claim of statistical superiority or comparative fatigue life was made. A true fatigue-life analysis would require a larger number of specimens, standardized censoring or failure endpoints, and testing of all specimens to the same predefined maximum cycle count or to complete structural failure.

### F. Inspection Decision Rules and Reproducibility Considerations

To reduce ambiguity in interpreting the visual observations, the inspection sequence was organized around mutually exclusive structural outcomes. A specimen could be free of abnormality, exhibit visible microdeformation without loss of function, develop permanent deformation, show crack or delamination, or demonstrate functional or structural failure. The laboratory report classified microdeformation as an abnormality but not as failure when the heel, ankle, fit, and overall function remained intact. This distinction was retained in the manuscript because conflating early deformation with failure would overstate the severity of the observation. The comparative endpoint was defined a priori as the first documented cycle at which visible microdeformation was noted. For specimens without microdeformation, the endpoint was right-censored at the last observed cycle. This framework allows the present data to be understood as early-response screening rather than classical fatigue-life estimation. In a larger study, the same structure could be extended to survival analysis using time-to-

**Table 2. Target cyclic fatigue-testing parameters and recorded experimental loading conditions, including minimum and maximum force, actual peak force, loading frequency, and predefined microdeformation stopping criterion.**

| Parameter | Value | Unit |
|---|---|---|
| Test mode | Cyclic/fatigue | - |
| Minimum target load | 50 | N |
| Maximum target load | 1,330 | N |
| Recorded maximum load | 1,460* | N |
| Frequency | 1 | Hz |
| Stop criterion | Visible microdeformation | - |

**Recorded actual peak force; it exceeded the 1,330 N target maximum by approximately 9.8% (δF = [(1,460 − 1,330)/1,330] × 100%). The same recorded maximum was documented for all six specimens, so the overshoot affected both groups equally; it is treated as a methodological deviation (Sections II.C and IV.E). The recorded minimum force was not available.*

Manuscript Received 16 September 2026; Accepted: 10 November 2026; Published online: 20 November 2026
**Digital Object Identifier (DOI):** https://doi.org/10.35882/jeeemi.v9i1.1921
**Copyright** © 2026 by the authors. Published by Jurusan Teknik Elektromedik, Politeknik Kesehatan Kemenkes Surabaya Indonesia. This work is an open-access article and licensed under a Creative Commons Attribution-ShareAlike 4.0 International License (CC BY-SA 4.0).

**Table 3. Operational definitions, visual inspection criteria, and analytical classification of structural responses during cyclic fatigue testing, distinguishing microdeformation, permanent deformation, material damage, functional failure, and right-censored observations.**

| Observation | Operational interpretation | Analytical role |
|---|---|---|
| No abnormality | No visible structural change; fit/function preserved | Censored at last observed cycle |
| Microdeformation | Visible local shape change without crack, permanent gross deformation, or functional loss | Primary endpoint |
| Permanent deformation | Persistent gross shape change after unloading | Secondary structural damage |
| Crack/delamination | Visible material separation or cracking | Secondary damage/failure indicator |
| Functional failure | Loss of fit, attachment, or structural function | Definitive failure |

event methods, with complete structural failure as a later endpoint and microdeformation as an intermediate event.

Reproducibility also depends on calibration and documentation of the loading system. The laboratory record included target minimum and maximum loads, frequency, actual maximum load, cycle counts, stopping criterion, pre-test condition, post-test condition, and photographic documentation. However, sensor calibration certificates, displacement traces, and continuous force-time records were not available in the research dataset. These omissions do not invalidate the descriptive observations but limit metrological characterization of the test. The operational definitions and analytical roles assigned to each structural observation are presented in Table 3.

### G. Mathematical Formulation of Loading, Response, Endpoints, and Uncertainty

The equations below formalize the quantities used in this study. To avoid introducing results that cannot be supported by the laboratory records, the role of each equation is stated explicitly: Eqs. (1)–(10) and (26)–(28) were evaluated using the recorded test parameters or specimen-level outcomes, whereas Eqs. (11)–(25) define the structural and metrological quantities that govern the observed response but could not be evaluated, because displacement, strain, cross-sectional geometry, material constants, and calibration data were not recorded. The latter equations specify the measurements required in a confirmatory study and clarify the interpretation of the present observations.

1. Cyclic loading parameters (evaluated)

$$F_c(t) = F_{\mathrm{m}} + F_{\mathrm{a}} \sin(2\pi f t) \quad (1)$$

where $F_c(t)$ is the pulsating test force applied alternately to the heel and forefoot (N), $F_{\mathrm{m}}$ is the mean force (N), $F_{\mathrm{a}}$ is the force amplitude (N), $f$ is the loading frequency (Hz), and $t$ is time (s). The sinusoidal pulsating force in Eq. (1) [24], [41] is the cyclic-loading form described in ISO 10328 and used in previous prosthetic-foot testing. The mean force, amplitude, force range, and load ratio are defined in Eqs. (2)–(5) [45] as

$$F_{\mathrm{m}} = \frac{F_{\max}+F_{\min}}{2} \quad (2)$$

$$F_{\mathrm{a}} = \frac{F_{\max}-F_{\min}}{2} \quad (3)$$

$$\Delta F = F_{\max} - F_{\min} = 2F_{\mathrm{a}} \quad (4)$$

$$R = \frac{F_{\min}}{F_{\max}} \quad (5)$$

where $F_{\max}$ and $F_{\min}$ are the upper and lower forces of the loading cycle (N), $\Delta F$ is the force range (N), and $R$ is the dimensionless load ratio. For the target settings ($F_{\min}$ = 50 N and $F_{\max}$ = 1,330 N), Eqs. (2)–(5) give $F_{\mathrm{m}}$ = 690 N, $F_{\mathrm{a}}$ = 640 N, $\Delta F$ = 1,280 N, and $R$ = 0.038. The deviation of the recorded peak from the target peak was quantified using Eq. (6) [24], [45] as

$$\delta_F = \frac{F_{\max,\mathrm{rec}}-F_{\max,\mathrm{tgt}}}{F_{\max,\mathrm{tgt}}} \times 100\% \quad (6)$$

where $F_{\max,\mathrm{rec}}$ is the recorded maximum force (1,460 N) and $F_{\max,\mathrm{tgt}}$ is the target maximum force (1,330 N), giving $\delta_F$ = 9.8%. The corresponding force amplitude under the recorded peak is given by Eq. (7) [45] as

$$F_{\mathrm{a,rec}} = \frac{F_{\max,\mathrm{rec}}-F_{\min}}{2} \quad (7)$$

Assuming that the lower force remained at the 50 N target, which could not be verified because the recorded minimum force was not available, $F_{\mathrm{a,rec}}$ = 705 N, i.e., 10.2% above the target amplitude; this value is therefore reported only as an upper-bound estimate.

2. Cycle exposure (evaluated)

$$N = f \cdot t \quad (8)$$

$$\eta = \frac{N_{\mathrm{obs}}}{N_{\mathrm{ISO}}} \times 100\% \quad (9)$$

$$N_{\mathrm{tot},g} = \sum_{i=1}^{n_g} N_i \quad (10)$$

Manuscript Received 16 September 2026; Accepted: 10 November 2026; Published online: 20 November 2026
**Digital Object Identifier (DOI):** https://doi.org/10.35882/jeeemi.v9i1.1921
**Copyright** © 2026 by the authors. Published by Jurusan Teknik Elektromedik, Politeknik Kesehatan Kemenkes Surabaya Indonesia. This work is an open-access article and licensed under a Creative Commons Attribution-ShareAlike 4.0 International License (CC BY-SA 4.0).

In Eqs. (8)–(10) [24], [45], $N$ is the number of cycles, $t$ is the loading time (s), $N_{obs}$ is the observed cycle count of a specimen, $N_{ISO}$ = 2,000,000 is the number of cycles prescribed for the P5 cyclic test [24], [40], [41], η is the exposure ratio (%), and $N_{tot,g}$ is the cumulative specimen-cycles of group $g$ containing $n_g$ specimens. At $f$ = 1 Hz, 10,000, 100,000, and 150,000 cycles correspond to 2.78 h, 27.8 h, and 41.7 h of loading and to η = 0.5%, 5.0%, and 7.5%, respectively.

3. Structural response quantities (defined; not evaluated)

The heel and forefoot forces act on inclined loading platforms. Their components normal and tangential to a platform inclined at angle γ are given by Eq. (11) [24], [44]

$$F_n = F\cos\gamma\,,\ F_s = F\sin\gamma \tag{11}$$

where γ = 15° for the heel and 20° for the forefoot in ISO 10328 [24], [40]. Because the platform angles actually used in the laboratory were not recorded, Eq. (11) was not evaluated. The local normal stress, engineering strain, and linear-elastic constitutive relation of a structural element are expressed by Eqs. (12)–(14) [44]

$$\sigma = \frac{F}{A} \tag{12}$$

$$\varepsilon = \frac{\Delta L}{L_0} \tag{13}$$

$$\sigma = E\varepsilon \tag{14}$$

where σ is the normal stress (MPa), $A$ is the load-bearing cross-sectional area (mm$^2$), ε is the engineering strain, Δ$L$ is the change in length (mm), $L_0$ is the initial length (mm), and $E$ is the elastic modulus (MPa). For the keel and dorsal shell, which act primarily in bending when forefoot load is applied at a distance from the ankle attachment, the bending moment and maximum bending stress are expressed by Eqs. (15) and (16) [44]

$$M = F \cdot d \tag{15}$$

$$\sigma_b = \frac{Mc}{I} \tag{16}$$

where $M$ is the bending moment (N·mm), $d$ is the moment arm between the line of action of the force and the section considered (mm), $c$ is the distance from the neutral axis to the outer fibre (mm), and $I$ is the second moment of area (mm$^4$). Eqs. (12)–(16) explain why a dorsal location is plausible for an early visible change, but they were not evaluated because the internal geometry and material constants of the commercial feet were unknown. The global stiffness and residual deformation of a foot, which provide an objective basis for defining microdeformation, are defined by Eqs. (17)–(19) [40], [41]

$$k = \frac{\Delta F}{\Delta s} \tag{17}$$

$$s_p = s_{\text{post}} - s_{\text{pre}} \tag{18}$$

$$\text{MD event if } s_p \geq s_{\text{th}} \tag{19}$$

where $k$ is the stiffness (N/mm), Δ$s$ is the displacement change of the loading platform corresponding to Δ$F$ (mm), $s_p$ is the residual deformation (mm) obtained from displacements measured at the 50 N reference load before ($s_{pre}$) and after ($s_{post}$) cycling, and $s_{th}$ is a predefined threshold. Eqs. (17)–(19) were not evaluated because displacement was not recorded; they are proposed as the quantitative replacement for the visual endpoint in future work.

4. Fatigue behaviour (defined; not evaluated)

$$\sigma_a = \sigma_f'\left(2N_f\right)^b \tag{20}$$

$$D = \sum \frac{n_i}{N_{f,i}} \tag{21}$$

Eq. (20) [49] is the Basquin stress–life relation, where $\sigma_a$ is the stress amplitude, $\sigma'_f$ is the fatigue strength coefficient, $N_f$ is the number of cycles to failure, and $b$ is the (negative) fatigue strength exponent [45], [49]. Eq. (21) [46] is the Palmgren–Miner cumulative damage rule, where $n_i$ is the number of cycles applied at stress level $i$, $N_{f,i}$ is the corresponding fatigue life, and failure is expected when $D \geq 1$ [45], [46]. Because $\sigma_a$ increases with $F_a$ and $b < 0$, Eq. (20) implies that the higher recorded amplitude reduces $N_f$; this qualitative implication supports the interpretation of the load overshoot given in Section II.C, whereas numerical life estimates were not attempted because $\sigma'_f$ and $b$ are unknown for the tested materials.

5. Measurement uncertainty (defined; not evaluated)

$$u_A = \frac{s}{\sqrt{n}} \tag{22}$$

$$u_B = \frac{a}{\sqrt{3}} \tag{23}$$

$$u_c = \sqrt{u_A^2 + \sum_j u_{B,j}^2} \tag{24}$$

$$U = k_p u_c \tag{25}$$

In Eqs. (22)–(25) [43], $u_A$ is the Type A standard uncertainty obtained from $n$ repeated readings with standard deviation $s$, $u_B$ is a Type B standard uncertainty for a quantity with half-width $a$ (e.g., load-cell accuracy or display resolution) under a rectangular distribution, $u_c$ is the combined standard uncertainty, and $U$ is the expanded uncertainty with coverage factor $k_p$ = 2 (approximately 95% coverage) [43]. Because calibration certificates and repeated force readings were not available, the uncertainty of the recorded

Manuscript Received 16 September 2026; Accepted: 10 November 2026; Published online: 20 November 2026
**Digital Object Identifier (DOI):** https://doi.org/10.35882/jeeemi.v9i1.1921
**Copyright** © 2026 by the authors. Published by Jurusan Teknik Elektromedik, Politeknik Kesehatan Kemenkes Surabaya Indonesia. This work is an open-access article and licensed under a Creative Commons Attribution-ShareAlike 4.0 International License (CC BY-SA 4.0).

1,460 N peak could not be quantified, and this is acknowledged as a metrological limitation.

6. Endpoint and censoring analysis (evaluated)

$$\hat{p} = \frac{x}{n} \quad (26)$$

$$\mathrm{CI} = \frac{\hat{p}+\frac{z^2}{2n} \pm z\sqrt{\frac{\hat{p}(1-\hat{p})}{n}+\frac{z^2}{4n^2}}}{1+\frac{z^2}{n}} \quad (27)$$

$$\hat{S}(N) = \prod_{N_i \le N}\left(1-\frac{d_i}{n_i}\right) \quad (28)$$

In Eqs. (26)–(28) [47], [48], $\hat{p}$ is the observed event proportion, $x$ is the number of specimens reaching the endpoint, $n$ is the number of specimens in the group, $CI$ is the Wilson score interval with $z$ = 1.96 for 95% confidence, which remains valid when $x$ = 0 or $x$ = $n$ [48], and $\hat{S}(N)$ is the Kaplan–Meier estimate of the proportion of specimens remaining free of the endpoint at cycle $N$, with $d_i$ events among $n_i$ specimens at risk at cycle $N_i$; specimens without an event contribute right-censored observations at their last observed cycle [47]. Eqs. (26)–(28) are descriptive and were not used for hypothesis testing.

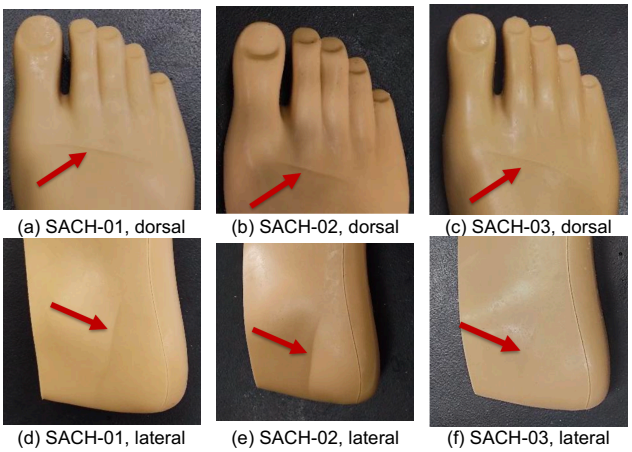



**Fig. 4. Representative post-test photographs of Group B SACH prosthetic feet (SACH-01, SACH-02, and SACH-03), comprising (a)–(c) dorsal forefoot views and (d)–(f) lateral views, showing localized dorsal and lateral microdeformation identified at 10,000 loading cycles. Red arrows indicate the visually observed deformation regions. The marked abnormalities represent visible microdeformation, not structural failure.**

## III. Result

### A. Baseline Inspection and Test Exposure

All six specimens were new and free of visible cracks, delamination, permanent deformation, or fit abnormalities before testing. The paired nominal sizes were identical across groups, allowing size-matched descriptive comparison. The cyclic system recorded a maximum load of 1,460 N for every specimen. The total recorded cycle exposure differed because testing was endpoint-driven rather than based on a uniform fixed cycle target. SACH-02 and SACH-03 were stopped at 10,000 cycles after microdeformation was identified. SACH-01 also reached the microdeformation endpoint at 10,000 cycles but, because of the documented communication error, continued to 150,000 cycles. Group A specimens SACH-04, SACH-05, and SACH-06 were each observed through 100,000 cycles without failure or visible microdeformation. In numerical terms, six specimens (three per group, sizes 23R, 24R, and 25R) were tested under identical target settings of 50–1,330 N at 1 Hz, and all six recorded the same maximum load of 1,460 N (9.8% above the target). The cumulative exposure was 470,000 specimen-cycles: 170,000 for Group B (150,000 + 10,000 + 10,000) and 300,000 for

**Table 4. Specimen-level cyclic fatigue-testing outcomes showing total accumulated loading cycles, first observed microdeformation endpoint, right-censored observations, and structural failure status for Group A and Group B SACH prosthetic feet.**

| Specimen | Total cycles | First endpoint | Failure |
|---|---|---|---|
| SACH-01 | 150,000* | Microdeformation at 10,000 | No |
| SACH-02 | 10,000 | Microdeformation at 10,000 | No |
| SACH-03 | 10,000 | Microdeformation at 10,000 | No |
| SACH-04 | 100,000 | No abnormality through 100,000 | No |
| SACH-05 | 100,000 | No abnormality through 100,000 | No |
| SACH-06 | 100,000 | No abnormality through 100,000 | No |

**Protocol deviation: SACH-01 received an additional 140,000 cycles (from 10,000 to 150,000 cycles) beyond the predefined microdeformation endpoint because of a protocol communication error. These additional cycles were excluded from the comparative analysis; the comparative endpoint remained the first microdeformation at 10,000 cycles. Group A entries (SACH-04 to SACH-06) are right-censored at 100,000 cycles.*

Manuscript Received 16 September 2026; Accepted: 10 November 2026; Published online: 20 November 2026
**Digital Object Identifier (DOI):** https://doi.org/10.35882/jeeemi.v9i1.1921
**Copyright** © 2026 by the authors. Published by Jurusan Teknik Elektromedik, Politeknik Kesehatan Kemenkes Surabaya Indonesia. This work is an open-access article and licensed under a Creative Commons Attribution-ShareAlike 4.0 International License (CC BY-SA 4.0).

Group A (3 × 100,000). Of the Group B exposure, only 30,000 specimen-cycles (17.6%) were accrued up to the valid endpoint; the remaining 140,000 cycles resulted solely from the protocol deviation in SACH-01. At 1 Hz, the Group B endpoint of 10,000 cycles corresponds to 2.78 h of loading and 0.5% of the 2,000,000 cycles prescribed for P5 cyclic testing, whereas the Group A observation limit of 100,000 cycles corresponds to 27.8 h and 5.0% of that cycle count.

### B. Microdeformation and Structural Integrity

Visible microdeformation was identified in all three Group B specimens at 10,000 cycles. The abnormality was located on the dorsal region of the prosthetic foot. Representative post-test photographs showing the visible microdeformation identified in the Group B specimens are presented in Fig. 4. In contrast, none of the Group A specimens showed comparable microdeformation through 100,000 cycles. Thus, the early structural endpoint was consistently different between the tested groups under the applied protocol.

Despite the presence of microdeformation in Group B, the laboratory did not classify any specimen as a structural failure. Across all six feet, there was no crack or delamination, no permanent gross deformation, no deterioration of the heel material or ankle region, and no functional or fitting abnormality after testing. These observations distinguish early surface or shell response from clinically consequential structural breakdown. The specimen-level cycle exposure, first observed structural endpoint, and failure status are presented in Table 4.

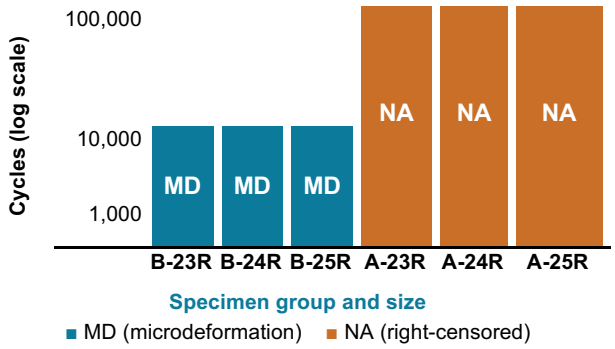



**Fig. 5. Comparison of the first observed structural endpoints among six commercial SACH prosthetic feet. MD indicates visible microdeformation at 10,000 cycles in Group B, whereas NA indicates no observed abnormality through 100,000 cycles in Group A. Group A observations are right-censored and do not represent confirmed fatigue-life values. Plotted values show the cycle count at the first observed endpoint (or the last observed cycle for censored specimens) rather than total accumulated cycles; SACH-01 (B-23R) accumulated 150,000 cycles in total because of a protocol deviation.**

### C. Summary of Group-Level Response

At the group level, the pattern was internally consistent: 3 of 3 Group B specimens developed visible microdeformation at 10,000 cycles, while 0 of 3 Group A specimens showed microdeformation through 100,000 cycles. The specimen-level distribution of the first structural endpoint further demonstrates this descriptive separation between the two commercial groups, as shown in Fig. 5. Because the exposure thresholds differed after the primary endpoint and the sample size was very small, the result is best interpreted as a marked descriptive separation in early observable structural response rather than a statistically established difference in fatigue life. Three observation types must be distinguished when interpreting these results. First, Group B specimens SACH-02 and SACH-03 each contributed an event at 10,000 cycles and were stopped at that point. Second, SACH-01 also contributed an event at 10,000 cycles; its continuation to 150,000 cycles was caused by a protocol communication error, and the post-endpoint cycles were not used in the comparison. Third, Group A specimens SACH-04, SACH-05, and SACH-06 contributed right-censored observations at 100,000 cycles, meaning that their endpoint, if any, lies beyond the final observation limit and remains unknown. Using Eq. (26), the observed event proportion was 3/3 (100%) for Group B and 0/3 (0%) for Group A. The corresponding 95% Wilson intervals from Eq. (27) were 43.9%–100% and 0%–56.1%, respectively; these intervals overlap, confirming that a sample of three specimens per group cannot support a statistically established difference. The Kaplan–Meier estimate from Eq. (28) fell from 1.00 to 0 at 10,000 cycles for Group B, whereas it remained at 1.00 up to the censoring limit of 100,000 cycles for Group A. Across all six specimens, 3 of 6 (50%) reached the microdeformation endpoint, and 0 of 6 (0%) developed cracking, delamination, permanent gross deformation, loss of fit, or structural failure. The absence of cracking, delamination, permanent deformation, and functional impairment in both groups indicates that the observed microdeformation represented an early abnormality rather than catastrophic failure. The finding is therefore relevant to screening and quality control, but it does not establish the clinical service life of either product group.

### D. Post-test Inspection Matrix

The post-test inspection matrix confirmed that the between-group difference was restricted to visible microdeformation. Heel material and ankle condition remained acceptable in all specimens. No cracks or delamination, no permanent deformation, and no loss of functional fit were reported. This consistency is important because it indicates that the observed Group B change represented an early local response rather

Manuscript Received 16 September 2026; Accepted: 10 November 2026; Published online: 20 November 2026
**Digital Object Identifier (DOI):** https://doi.org/10.35882/jeeemi.v9i1.1921
**Copyright** © 2026 by the authors. Published by Jurusan Teknik Elektromedik, Politeknik Kesehatan Kemenkes Surabaya Indonesia. This work is an open-access article and licensed under a Creative Commons Attribution-ShareAlike 4.0 International License (CC BY-SA 4.0).

**Table 5. Comparative post-test structural inspection results for Group A and Group B SACH prosthetic feet, including overall condition, heel integrity, ankle condition, cracking, delamination, microdeformation, functional fit, and structural failure.**

| Inspection item | Group B | Group A |
|---|---|---|
| Overall visual condition | Microdeformation present | No visible abnormality |
| Heel material | Good | Good |
| Ankle region | Good | Good |
| Crack/delamination | None | None |
| Permanent deformation | None | None |
| Microdeformation | 3/3 specimens | 0/3 specimens |
| Function/fit | Good | Good |
| Structural failure | None | None |

than generalized structural breakdown. A complete group-level summary of the post-test structural inspection findings is provided in Table 5.

## IV. Discussion

This Discussion integrates four components: interpretation of the principal findings (Sections IV.A, IV.B, and IV.H), comparison with previous studies (Sections IV.C and IV.G), methodological weaknesses and limitations (Sections IV.E and IV.N), and engineering and practical implications for laboratory screening and prosthetic-component evaluation (Sections IV.D, IV.F, IV.I, IV.L, and IV.M).

### A. Principal Findings

This study provides preliminary comparative evidence that two commercially supplied SACH foot groups can demonstrate substantially different early responses to repeated mechanical loading even when their external form and nominal sizes are similar. The central finding was that visible microdeformation appeared at 10,000 cycles in every Group B specimen, whereas Group A specimens remained free of the same abnormality through 100,000 cycles. Importantly, no complete structural failure occurred in either group, and all specimens retained heel integrity, ankle integrity, functional fit, and freedom from crack or delamination.

The result should be interpreted at the level of early mechanical response. It does not demonstrate that Group A has a quantified fatigue life ten times longer than Group B. Such an inference would be invalid because Group B specimens met the predefined visual endpoint at 10,000 cycles, Group A specimens were observed only to 100,000 cycles, and none of the specimens were systematically tested to complete failure. The protocol deviation in SACH-01 further reinforces the importance of separating first endpoint from total accumulated cycles.

### B. Mechanical Interpretation

A SACH foot is mechanically simple compared with articulated or energy-storing designs, yet its behavior remains dependent on geometry, constituent materials, local stiffness, interfaces, and manufacturing consistency. Finite element and experimental studies have shown that changes in keel geometry, polymer selection, reinforcement, and external shell properties can alter stress distribution and deformation [26]. The present study did not characterize the internal materials of the two commercial groups, so the mechanism responsible for the observed difference cannot be assigned to a specific material property.

Several plausible engineering factors warrant investigation. Variability in foam density, shell thickness, keel stiffness, adhesive bonding, internal reinforcement, or molding consistency could change the manner in which repeated loads are transmitted from the connector to the heel and forefoot. Studies of polymer, rubber, wood, and composite structures demonstrate that material interfaces and processing conditions can meaningfully affect deformation, stiffness, and fatigue-related damage [27], [29], [32], [33]. These factors are especially relevant in low-cost components where production tolerances may not be fully described in publicly available technical documentation. The dorsal location of the microdeformation is also mechanically plausible because local bending and shell deformation can develop as cyclic loads are transferred through the internal keel and compliant external structure. However, without digital image correlation, strain measurement, hardness testing, or destructive post-test inspection, the present data cannot determine whether the visible change originated in the external foam, internal keel, bonding layer, or another component.

### C. Comparison with Previous Prosthetic-Foot Research

The findings complement recent work emphasizing objective mechanical evaluation of affordable prosthetic feet. Nugroho et al. demonstrated that polymer-keel configuration affected deformation and load distribution in a SACH foot under ISO 10328-based loading, supporting the principle that apparently small structural differences can produce measurable changes in mechanical performance [1]. Balaramakrishnan et al. similarly reported experimentally validated relationships between design

Manuscript Received 16 September 2026; Accepted: 10 November 2026; Published online: 20 November 2026
**Digital Object Identifier (DOI):** https://doi.org/10.35882/jeeemi.v9i1.1921
**Copyright** © 2026 by the authors. Published by Jurusan Teknik Elektromedik, Politeknik Kesehatan Kemenkes Surabaya Indonesia. This work is an open-access article and licensed under a Creative Commons Attribution-ShareAlike 4.0 International License (CC BY-SA 4.0).

configuration, deformation, stress, and energy behavior in prosthetic feet [3].

Falbriard et al. developed and tested an affordable dynamic prosthetic foot and highlighted the need to balance mechanical function, accessibility, and manufacturability [4]. Abdalwahhab and colleagues used mechanical analysis and fatigue testing to investigate flexible-keel and non-articulated feet, showing that repetitive loading can expose durability differences that are not apparent from static inspection [11], [25]. Worajinda et al. combined experimental validation and finite element modelling for a composite SACH foot, further demonstrating the value of integrated structural evaluation [13]. A quantitative comparison with previous studies must account for substantial methodological differences. Jensen and Treichl performed 1,132 ISO 10328 tests on 21 prosthetic-foot models used in low-income countries; none passed the strictest protocol, all but one failed the initial static proof test at 2,240 N because of permanent forefoot deformation, and non-Jaipur rubber feet showed a mean permanent forefoot deformation of 8.3 ± 3.4 mm against the optional 5 mm ISO limit [40]. Mason et al. reported that heavy-duty commercial feet passed P5 cyclic testing between 50 N and 1,330 N at 1 Hz for 2,000,000 cycles, although stiffness and creep changed significantly within some models after cycling [41]. Sasaki et al. completed 2,000,000 cycles at 1.28 kN and 1 Hz on a modified natural-rubber SACH foot, with maximum forefoot and heel displacements of 32.03 mm and 8.77 mm [42]. Abdalwahhab et al. used a pneumatic heel-and-forefoot fatigue tester at an applied load of approximately 870 N and reported failure of a SACH foot at 473,241 cycles, compared with 510,382 cycles for a flexible-keel foot [25]. Nugroho et al. reported a mean deformation of 20.12 mm, a maximum stress of 12.67 MPa, and a safety factor of 1.59 for a polymer-keel SACH foot validated statically up to 1,176.78 N, with FEA–experiment deviations below 5% [1].

Against this background, the first Group B event at 10,000 cycles corresponds to only 0.5% of the 2,000,000 cycles prescribed for P5 cyclic testing, under a recorded peak of 1,460 N that was 9.8% above the P5 cyclic level used in [40], [41] and 14.1% above the 1.28 kN level used in [42], but 34.8% below the 2,240 N static proof load [40]. The Group A observation limit of 100,000 cycles corresponds to 5.0% of the ISO cycle count and to approximately 21% of the 473,241 cycles to failure reported for a SACH foot under a lower load of approximately 870 N [25]. These values are not equivalent to cycles to failure in [25] or to pass/fail outcomes in [40], [41], [42], because the present test was stopped at a visual early endpoint, used no displacement measurement, and did not complete the prescribed cycle count. The comparison therefore supports only two qualitative similarities: as in [40], deformation-related changes rather than fracture were the predominant early response of SACH-type feet, and, as in [41], externally similar commercial feet can differ in their response to cyclic loading. The main difference is that the present study compared finished commercial products from the same procurement channel, whereas the cited studies addressed prototype development, single reference feet, or certification-oriented testing.

The present study differs from those design-development studies because it examined finished commercial products without modifying their structure. This distinction is important for clinical engineering and procurement. Rehabilitation services frequently select components from available inventories rather than from fully characterized research prototypes. A simple, reproducible cyclic-screening protocol can therefore serve as a practical quality-assurance step before large-scale procurement or distribution.

### D. Relevance to Rehabilitation Engineering and Component Selection

Mechanical screening of prosthetic components has direct relevance to rehabilitation engineering. Foot stiffness and structural response can influence loading patterns, perceived behavior, and gait biomechanics [5], [12], [22], [23], [34]. Nevertheless, mechanical durability is only one dimension of prosthetic-foot selection. Clinical prescription must also consider body mass, activity level, cadence, terrain, alignment, footwear, comfort, user goals, and cost. The present results therefore should not be interpreted as a clinical recommendation that one commercial group is universally preferable to another. Instead, the study supports a quality-assurance principle: internal inventory labels should not substitute for objective performance data. The Group A and Group B designations used in this study were merely internal codes, not manufacturer-certified engineering grades. A stronger procurement framework would request traceable information on material composition, rated user mass, proof-load limits, fatigue-cycle performance, stiffness characteristics, environmental durability, and standardized failure criteria. Where such information is absent, independent laboratory screening may reduce uncertainty. The broader literature on additive manufacturing and alternative prosthetic materials also demonstrates that affordability and local manufacturability need not exclude rigorous engineering validation [14], [16], [17], [18], [19], [20], [34], [35], [36], [37], [38], [39]. Future low-cost prosthetic innovation should therefore integrate standardized mechanical testing from the earliest design and procurement stages rather than treating it as a post-development activity.

Manuscript Received 16 September 2026; Accepted: 10 November 2026; Published online: 20 November 2026
**Digital Object Identifier (DOI):** https://doi.org/10.35882/jeeemi.v9i1.1921
**Copyright** © 2026 by the authors. Published by Jurusan Teknik Elektromedik, Politeknik Kesehatan Kemenkes Surabaya Indonesia. This work is an open-access article and licensed under a Creative Commons Attribution-ShareAlike 4.0 International License (CC BY-SA 4.0).

### E. Interpretation of Load Overshoot and Test Standardization

The difference between the target maximum load of 1,330 N and the recorded maximum of 1,460 N requires explicit interpretation. The recorded peak was approximately 9.8% above the target. In pneumatic or servo-pneumatic cyclic systems, transient overshoot can occur depending on actuator response, regulator dynamics, damping, load-cell sampling, and contact conditions. The present dataset does not include the time-resolved force trace required to identify the mechanism, so no causal explanation is asserted. For internal comparison, the key mitigating factor is that the same recorded maximum load was reported for all six specimens. Thus, there is no evidence that one product group was systematically exposed to a higher peak than the other. Nevertheless, a future confirmatory study should include pre-test calibration, continuous force logging, acceptance tolerances for peak load, and automatic shutdown when the commanded load exceeds the allowable band. Such controls would strengthen both ISO traceability and the defensibility of between-group comparisons. The overshoot also illustrates why reporting only the nominal test setting can be misleading. Biomedical and rehabilitation engineering studies should distinguish commanded load, measured load, and failure criterion. This is particularly important when mechanical test data are later used to support procurement decisions or safety claims.

### F. Commercial Traceability and Quality-Assurance Implications

A notable feature of the present study is that the two product groups were identified by internal codes rather than by a standardized manufacturer grading system. This reflects a real-world problem in low-cost component procurement: inventory labels may become proxies for perceived quality even when the underlying engineering specification is not fully documented. From a quality-management perspective, this creates a traceability gap. A robust prosthetic-component procurement record should ideally include manufacturer, model, production batch, material declaration, recommended user mass, activity classification, test standard, static proof-load rating, fatigue-cycle rating, environmental limits, and warranty information. When these data are absent, internal labels should be treated as logistical identifiers only. The present manuscript therefore intentionally avoids phrases such as 'premium grade' or 'higher-quality material' because the available evidence does not support those claims.

The observed difference in early cyclic response suggests that inventory categories can warrant

**Table 6. Comparison of specimen characteristics, experimental loading conditions, testing methods, fatigue endpoints, and quantitative mechanical outcomes between the present investigation and previously published prosthetic-foot studies.**

| Study | Specimens and test conditions | Load and cycles | Endpoint and numerical outcome |
|---|---|---|---|
| Nugroho et al. [1] | Polymer-keel SACH prototype; FEA + static test | Static, up to 1,176.78 N | Deformation 20.12 mm; stress 12.67 MPa; safety factor 1.59; FEA error < 5% |
| Worajinda et al. [13] | Composite SACH (nylon keel, PU foam); FEA + static ISO 10328:2016 test | Static loading at several angles | Mean FEA error < 15.22% |
| Abdalwahhab et al. [25] | SACH vs flexible-keel foot; pneumatic fatigue tester | ≈ 870 N; tested to failure | Failure at 473,241 cycles (SACH) vs 510,382 cycles (flexible keel) |
| Jensen and Treichl [40] | 21 foot models used in low-income countries; ISO 10328 battery | Proof 2,240 N; cyclic 50–1,330 N | None passed strictest protocol; permanent forefoot deformation 8.3 ± 3.4 mm (rubber, non-Jaipur) |
| Mason et al. [41] | Heavy-duty commercial feet, 3 manufacturers; ISO 10328 P5 | 50–1,330 N, 1 Hz, 2,000,000 cycles | All passed; significant within-model changes in stiffness and creep |
| Sasaki et al. [42] | Modified natural-rubber SACH; cyclic part of ISO 10328 | 1.28 kN, 1 Hz, 2,000,000 cycles | Completed; maximum displacement 32.03 mm (forefoot) and 8.77 mm (heel) |
| Present study | 6 finished commercial SACH feet (3 vs 3), size-matched; visual endpoint | 50–1,330 N target (1,460 N recorded), 1 Hz; endpoint-driven | Group B: 3/3 microdeformation at 10,000 cycles; Group A: 0/3 through 100,000 cycles (censored); no failure |

Manuscript Received 16 September 2026; Accepted: 10 November 2026; Published online: 20 November 2026
**Digital Object Identifier (DOI):** https://doi.org/10.35882/jeeemi.v9i1.1921
**Copyright** © 2026 by the authors. Published by Jurusan Teknik Elektromedik, Politeknik Kesehatan Kemenkes Surabaya Indonesia. This work is an open-access article and licensed under a Creative Commons Attribution-ShareAlike 4.0 International License (CC BY-SA 4.0).

independent verification. However, the correct engineering response is not to generalize from three specimens to all future units. Instead, the result should trigger batch-level characterization, incoming inspection, documentation requirements, and periodic mechanical audit. This approach aligns prosthetic procurement with broader principles of medical-device quality assurance and risk control.

### G. Comparison Matrix with Recent Mechanical Studies

The methodological position of the present study relative to selected recent prosthetic-foot mechanical investigations is summarized in Table 6. Most prior studies focused on design optimization, finite element analysis, or prototype validation. The current contribution is narrower but complementary: it evaluates finished commercial SACH feet as a quality-assurance problem using cyclic loading and a predefined visual endpoint.

### H. Engineering Significance of Microdeformation as an Early Endpoint

Microdeformation deserves specific attention because it occupies an intermediate position between normal elastic response and overt structural failure. A prosthetic foot is expected to deform elastically during loading, but the external shape should recover when load is removed. A persistent or visually detectable local change may indicate material set, localized yielding, interface slip, or progressive damage even when gross function remains intact. For this reason, early deformation can be useful as a screening signal in quality assurance, particularly when the objective is to identify products that merit further testing rather than to certify definitive service life. The distinction between elastic deformation, microdeformation, and permanent structural deformation should be standardized in future work. Elastic deformation should be quantified during loading and recovery; microdeformation should be defined by a reproducible displacement or surface-profile threshold; and permanent deformation should be confirmed after a defined unloading and recovery interval. The present visual endpoint was adequate for exploratory screening but cannot provide the metrological resolution required for certification or design optimization. The consistent timing of microdeformation in all three Group B specimens at 10,000 cycles is noteworthy because it reduces the likelihood that the finding arose from a single isolated specimen. Nevertheless, three observations remain insufficient to characterize batch variation or estimate a probability of failure. Replication across independent production lots is essential before the observed pattern can be generalized.

**Table 7. Proposed six-stage quality-assurance framework for commercial SACH prosthetic feet, describing specimen traceability, baseline inspection, static screening, cyclic testing, quantitative assessment, and final disposition, together with the recommended documentation.**

| Stage | Minimum action | Key record |
|---|---|---|
| 1. Traceability | Record manufacturer/model or internal code, batch, size, side, receipt date | Specimen identity and provenance |
| 2. Baseline inspection | Inspect shell, heel, ankle, connector, dimensions, visible defects | Photographs and inspection checklist |
| 3. Static screening | Apply controlled proof load within rated range | Commanded and measured load |
| 4. Cyclic testing | Apply repeat loading with defined frequency and tolerance | Cycle count, force trace, stop criterion |
| 5. Quantitative inspection | Measure deformation, stiffness, hardness, or surface geometry | Pre/post numerical values |
| 6. Disposition | Classify pass, conditional pass, investigate, or fail | Signed technical decision |

### I. Proposed Quality-Assurance Pathway for Commercial SACH Feet

The study supports a staged quality-assurance pathway that can be implemented by prosthetic service providers, distributors, or academic laboratories. Stage 1 should establish product traceability, including manufacturer, model, batch, size, side, date of receipt, and technical documentation. Stage 2 should include baseline dimensional and visual inspection. Stage 3 should perform static proof loading within the rated range. Stage 4 should apply cyclic loading with controlled force tolerance and predefined intermediate inspection points. Stage 5 should quantify post-test changes using objective metrology. Stage 6 should

Manuscript Received 16 September 2026; Accepted: 10 November 2026; Published online: 20 November 2026
**Digital Object Identifier (DOI):** https://doi.org/10.35882/jeeemi.v9i1.1921
**Copyright** © 2026 by the authors. Published by Jurusan Teknik Elektromedik, Politeknik Kesehatan Kemenkes Surabaya Indonesia. This work is an open-access article and licensed under a Creative Commons Attribution-ShareAlike 4.0 International License (CC BY-SA 4.0).

document disposition as pass, conditional pass, further investigation, or failure. Such a pathway is especially useful where procurement decisions are driven by affordability and availability. Low cost should not be equated with low quality, but neither should low-cost components be assumed equivalent without evidence. Engineering screening can help separate procurement risk from price alone and can provide feedback to suppliers about recurrent structural abnormalities. The process also creates a traceable evidence base for future clinical monitoring. For clinical engineering departments, the minimum documentation package should include the commanded and measured load, cycle count, frequency, loading geometry, fixture configuration, calibration status, environmental conditions, inspection intervals, endpoint definition, and photographic evidence. If a specimen reaches an early abnormality, the event should be time-stamped by cycle count and confirmed independently by a second observer or measurement method. This structure would reduce ambiguity, such as the communication-related continuation that occurred for SACH-01 in the present study. The proposed six-stage quality-assurance pathway and the minimum documentation required at each stage are summarized in Table 7.

### J. Generalizability and Clinical Translation

The generalizability of the findings is deliberately limited. The results apply directly only to the six tested specimens and the laboratory conditions used. They should not be extrapolated to every SACH foot manufactured in the same country, every product sold under similar internal codes, or every user profile. Commercial supply chains can change material sources, tooling, vendors, and production batches without visible changes to the external product. Clinical translation requires additional steps because laboratory cyclic response and patient experience are not interchangeable outcomes. A component that shows no bench abnormality may still be uncomfortable, excessively stiff, poorly aligned, or unsuitable for a specific activity level. Conversely, a localized shell change may have limited clinical consequence if it does not progress or alter load transfer. Longitudinal field studies should therefore combine mechanical surveillance with gait outcomes, user-reported comfort, daily wear time, activity monitoring, maintenance events, and component replacement records. A useful translational design would enroll users only after candidate components pass standardized bench screening, then track performance prospectively. The laboratory endpoint could be correlated with clinical wear, socket-prosthesis alignment, body mass, cadence, terrain exposure, and eventual replacement. This would allow engineering observations to be linked to clinically meaningful reliability instead of assuming that cycle count alone represents real-world lifespan.

### K. Strengths of the Study

Despite its exploratory design, the study has several strengths. First, it used size-matched specimens across two commercial groups, reducing one obvious source of geometric confounding. Second, all specimens were new and underwent pre-test inspection. Third, the same laboratory, apparatus, frequency, target load settings, and observation framework were used for both groups. Fourth, the abnormality was documented photographically and localized to a consistent dorsal region in all Group B specimens. Fifth, the manuscript distinguishes internal inventory coding from manufacturer grading and explicitly reports protocol deviations rather than masking them. The study also addresses an underreported translational question. Prosthetic engineering literature often emphasizes novel devices, materials, or numerical optimization, whereas clinicians and service providers also need methods to evaluate commercially available components already entering routine supply chains. Preliminary bench screening can identify products or batches that warrant deeper mechanical characterization before widespread clinical use.

### L. Clinical Engineering and Procurement Decision-Making

From a clinical-engineering perspective, the value of the present study lies in converting an informal product distinction into a testable engineering question. Procurement teams often work under constraints of price, availability, reimbursement, import lead times, and urgent patient needs. These pressures may encourage reliance on supplier descriptions or internal inventory experience. Mechanical screening provides a structured counterbalance by generating observable evidence before a component is distributed more widely. The current findings are insufficient to justify excluding Group B from procurement, because the clinical significance and progression of the observed microdeformation remain unknown. A proportionate response would be to classify Group B as requiring additional verification. This could include retesting specimens from multiple batches, quantifying deformation, obtaining manufacturer documentation, and monitoring field replacements. Group A similarly should not be considered certified or superior solely because no abnormality was observed through 100,000 cycles. Its true fatigue limit was not established.

A procurement decision should therefore combine at least four evidence domains: technical documentation, independent mechanical testing, clinical suitability, and lifecycle cost. Technical documentation addresses traceability and rated performance; mechanical testing addresses structural behavior; clinical suitability addresses user-specific

Manuscript Received 16 September 2026; Accepted: 10 November 2026; Published online: 20 November 2026
**Digital Object Identifier (DOI):** https://doi.org/10.35882/jeeemi.v9i1.1921
**Copyright** © 2026 by the authors. Published by Jurusan Teknik Elektromedik, Politeknik Kesehatan Kemenkes Surabaya Indonesia. This work is an open-access article and licensed under a Creative Commons Attribution-ShareAlike 4.0 International License (CC BY-SA 4.0).

prescription; and lifecycle cost incorporates purchase price, replacement frequency, maintenance, and service interruptions. A component with a low initial purchase price may prove less economical if it requires frequent replacement, whereas a more durable component may still be inappropriate if its stiffness or geometry is poorly matched to the user's needs. For prosthetic service providers, the proposed evidence framework can support transparent communication with patients and payers. Rather than presenting product categories as inherently 'better' or 'worse,' clinicians can explain that components have different mechanical characteristics, evidence levels, and intended use conditions. This language is more consistent with evidence-based prescription and avoids converting internal commercial labels into unsupported quality claims.

minimum of several specimens from at least three production batches would be preferable to three single-batch specimens, although the final sample size should be based on pilot variance and the intended statistical comparison. Randomized test order would reduce temporal equipment effects. Investigators should predefine acceptable load tolerance, for example a narrow percentage band around the target, and use automated acquisition to record force, displacement, and cycle count continuously.

Objective deformation measurement is essential. Digital image correlation can quantify full-field displacement and strain without physical contact, while 3D scanning can characterize persistent surface changes before and after cycling [30]. Load-displacement curves can quantify stiffness and hysteresis, and hardness testing can detect changes in

**Table 8. Recommended methodological requirements for future confirmatory SACH prosthetic-foot fatigue studies, covering specimen sampling, loading control, endpoint definition, instrumentation, statistical analysis, and clinical validation.**

| Domain | Recommended specification | Purpose |
|---|---|---|
| Sampling | Multiple specimens from multiple production batches | Estimate within- and between-batch variability |
| Loading control | Continuous measured force with predefined tolerance | Prevent undocumented overshoot and ensure comparability |
| Endpoints | Quantified microdeformation, permanent deformation, and structural failure | Separate early damage from definitive failure |
| Instrumentation | Force, displacement, cycle logging; DIC or 3D scanning where available | Quantify structural response objectively |
| Analysis | Time-to-event or repeated-measures models with effect sizes and confidence intervals | Support defensible group comparison |
| Translation | Prospective field surveillance after bench screening | Link laboratory response to clinical service life |

### M. Recommended Confirmatory Fatigue-Test Protocol

A confirmatory study should begin with an a priori protocol that separates screening endpoints from definitive failure endpoints. The primary fatigue endpoint could be structural failure or a quantitatively defined permanent deformation threshold, while visible microdeformation could be retained as a secondary intermediate endpoint. All specimens should be tested under identical force limits, frequency, loading geometry, and environmental conditions. If a specimen reaches an intermediate endpoint, the protocol should specify whether testing stops, continues under observation, or transitions to a separate damage-progression phase.

The next study should also include sufficient replication to estimate within-group variability. A

compliant heel or shell material. Combined compression, flexural, and tensile testing supported by finite element analysis has also been used to characterize the mechanical performance of materials for customized orthoses [31], and a comparable multi-test approach could be applied to SACH-foot constituents. If the internal keel can be evaluated non-destructively, computed tomography or ultrasound may identify subsurface defects; otherwise, destructive sectioning after fatigue testing can reveal cracks, bond separation, or material set.

Statistical analysis should reflect the endpoint. Time-to-event methods are appropriate when specimens are tested until failure or censoring; repeated-measures models are appropriate when stiffness or deformation is measured at multiple cycle checkpoints; and mixed-effects models can account for

Manuscript Received 16 September 2026; Accepted: 10 November 2026; Published online: 20 November 2026
**Digital Object Identifier (DOI):** https://doi.org/10.35882/jeeemi.v9i1.1921
**Copyright** © 2026 by the authors. Published by Jurusan Teknik Elektromedik, Politeknik Kesehatan Kemenkes Surabaya Indonesia. This work is an open-access article and licensed under a Creative Commons Attribution-ShareAlike 4.0 International License (CC BY-SA 4.0).

batch-level clustering. Effect sizes and confidence intervals should be prioritized over binary significance testing, particularly when engineering relevance depends on magnitude rather than p-value alone. Finally, laboratory findings should be cross-validated against field performance. A prospective surveillance phase could record user body mass, mobility level, daily wear time, step counts, terrain exposure, maintenance, and time to component replacement. Correlating laboratory endpoints with real-world service events would allow fatigue testing to evolve from a purely bench-based procedure into a clinically meaningful predictive tool for prosthetic-component management. The principal methodological elements recommended for a future confirmatory SACH foot fatigue study are summarized in Table 8.

### N. Methodological Considerations and Limitations

The principal limitation is the small sample size of three specimens per group. The study should therefore be regarded as an exploratory bench comparison rather than confirmatory evidence about all products represented by the two internal codes. Second, microdeformation was identified visually and was not quantified using displacement sensors, digital image correlation, 3D scanning, strain gauges, or surface profilometry. Although the laboratory photographs document the abnormality, the magnitude of deformation cannot be expressed in millimeters or strain units. Third, the target maximum load was 1,330 N, but the recorded maximum load was 1,460 N for all specimens. This approximately 9.8% overshoot is an important test-system deviation. Because it was consistent across specimens, the internal comparison remains informative, but strict conformity with the intended target load cannot be claimed. Fourth, SACH-01 continued to 150,000 cycles after microdeformation had already been detected at 10,000 cycles because of a communication error. The analysis therefore used the first-detection cycle as the valid endpoint and treated the additional exposure as a protocol deviation rather than as evidence of durability.

Fifth, detailed manufacturer specifications, material composition, keel geometry, density, hardness, and batch-level production information were unavailable. The mechanism underlying the between-group difference therefore remains unknown. Finally, laboratory cyclic loading cannot fully reproduce the multiaxial and highly variable loads of daily prosthesis use. Real-world performance depends on user-specific and environmental conditions, and clinical service life cannot be extrapolated directly from the present cycle counts.

Additional weaknesses should be stated explicitly. The manufacturing batches and production dates of the six specimens were unknown; each group may therefore represent a single production lot, and between-batch variability could not be separated from between-group differences. The microdeformation endpoint was assessed subjectively by visual inspection without documented blinding, a second observer, or a calibrated measurement, so the detection threshold may differ between observers and laboratories. Displacement, stiffness, and continuous force–time data were not recorded, preventing quantification of deformation magnitude, stiffness change, or load uncertainty using Eqs. (17)–(25). Finally, the testing exposure was unequal: Group B specimens were evaluated to the 10,000-cycle endpoint (with one deviation to 150,000 cycles), whereas Group A specimens were observed to 100,000 cycles, which corresponds to only 5.0% of the 2,000,000 cycles prescribed by ISO 10328 for P5 testing.

These limitations influence interpretation in specific ways. The small sample and overlapping Wilson intervals mean that the 3/3 versus 0/3 contrast should be regarded as a consistent descriptive signal rather than a population estimate. The subjective endpoint means that the 10,000-cycle value indicates when an abnormality was first recognized, not when it physically began. The unequal and censored exposure means that neither group's fatigue life, nor the ratio between them, can be inferred, and the absence of testing to 2,000,000 cycles means that ISO 10328 conformity cannot be claimed for either group.

For practical application in prosthetic-foot quality assessment, the present protocol is best used as an incoming-inspection screening step that flags product groups requiring further verification, not as an acceptance or rejection criterion. A practical implementation would retain the same cyclic settings while adding a displacement transducer, a predefined residual-deformation threshold according to Eqs. (18) and (19), a second blinded observer, calibrated photographs, fixed inspection intervals, and documentation of batch numbers, so that a positive screening result can trigger confirmatory full ISO 10328 testing.

### O. Directions for Future Research

A definitive follow-up study should increase the number of specimens per commercial group, use batch-stratified sampling, and apply an identical pre-specified cycle limit or test every specimen to structural failure. Survival-type fatigue analysis could then estimate cycles to endpoint and compare failure distributions. Instrumented measurement should include force calibration, displacement, stiffness, hysteresis, hardness, and preferably digital image correlation or 3D surface scanning to quantify deformation.

Material characterization should examine the keel, foam or rubber shell, bonding interfaces, and

Manuscript Received 16 September 2026; Accepted: 10 November 2026; Published online: 20 November 2026
**Digital Object Identifier (DOI):** https://doi.org/10.35882/jeeemi.v9i1.1921
**Copyright** © 2026 by the authors. Published by Jurusan Teknik Elektromedik, Politeknik Kesehatan Kemenkes Surabaya Indonesia. This work is an open-access article and licensed under a Creative Commons Attribution-ShareAlike 4.0 International License (CC BY-SA 4.0).

attachment structure before and after fatigue exposure. Combining cyclic testing with finite element analysis would help identify stress concentrations corresponding to the observed dorsal deformation. Post-fatigue destructive analysis could determine whether visible microdeformation is associated with internal cracking, interface separation, or permanent material set. The engineering sequence should ultimately be linked to clinical validation. After laboratory screening establishes safety and structural consistency, gait analysis, user-reported comfort, activity monitoring, and longitudinal field use could determine whether laboratory differences translate into meaningful functional or service-life outcomes.

## V. Conclusion

This study aimed to compare the early observable cyclic mechanical response of two groups of finished commercial SACH prosthetic feet, identified only by internal inventory codes, under ISO 10328-based alternating heel and forefoot loading, and to establish a reproducible screening framework for such components.

Six size-matched specimens were loaded at a target range of 50–1,330 N and 1 Hz, with a recorded maximum load of 1,460 N (9.8% overshoot) for every specimen. All three Group B specimens (3/3, 100%) developed visible dorsal microdeformation at 10,000 cycles, which corresponds to 0.5% of the 2,000,000 cycles prescribed for P5 testing, whereas none of the three Group A specimens (0/3, 0%) showed a comparable abnormality through the 100,000-cycle observation limit (right-censored). One Group B specimen continued to 150,000 cycles only because of a protocol communication error, and its valid endpoint remained 10,000 cycles. No specimen developed cracking, delamination, permanent gross deformation, functional-fit impairment, or structural failure. The results demonstrate a consistent descriptive difference in early cyclic response under the applied protocol; however, the overlapping 95% Wilson intervals (43.9%–100% versus 0%–56.1%), the visual endpoint, the load overshoot, and the unequal exposure mean that neither comparative fatigue durability nor ISO 10328 conformity can be claimed.

Future research should (1) quantify deformation objectively with displacement transducers, digital image correlation, or 3D surface scanning and adopt a predefined residual-deformation threshold to replace the visual endpoint; (2) apply standardized cyclic testing with calibrated, continuously logged force, a predefined force tolerance, and an identical cycle limit of 2,000,000 cycles or testing to structural failure for all specimens; (3) test additional specimens drawn from several production batches to estimate within- and between-batch variability; (4) improve monitoring through fixed inspection intervals, blinded duplicate assessment, calibrated photographs, and automatic shutdown; and (5) link laboratory screening results with material characterization and longitudinal clinical field performance.

## Acknowledgments

The authors acknowledge the Mechatronics Laboratory, Faculty of Industrial Technology, Universitas Islam Indonesia, Yogyakarta, Indonesia, for providing mechanical testing facilities and technical assistance. The authors also acknowledge SAEP Orthotics and Prosthetics for facilitating access to the commercial SACH prosthetic-foot specimens used in this study.

## Funding

This research received no specific grant from any funding agency in the public, commercial, or not-for-profit sectors.

## Data Availability

The laboratory test report, de-identified specimen-level mechanical testing records, cyclic loading data, inspection results, and photographic documentation supporting the findings of this study are available from the corresponding author upon reasonable request. Certain experimental parameters, including continuous force–time traces, displacement measurements, and calibration certificates, were not available in the research records, as acknowledged in the manuscript.

## Code Availability

No custom software code was developed or used for the mechanical testing or primary data analysis. Any scripts used solely to generate descriptive graphical illustrations may be made available by the corresponding author upon reasonable request.

## Author Contributions

Mahfud Saifudin: Investigation, specimen preparation, data collection, experimental documentation, and writing original draft.
Nur Rachmat: Conceptualization, methodology, supervision, data interpretation, manuscript development, writing review and editing, and corresponding authorship.
Sisybania: Manuscript development and writing review and editing.
Anissa Eka Septiani: Manuscript development and writing review and editing.
All authors have read and approved the final manuscript and agree to be accountable for the accuracy and integrity of the research.

Manuscript Received 16 September 2026; Accepted: 10 November 2026; Published online: 20 November 2026
**Digital Object Identifier (DOI):** https://doi.org/10.35882/jeeemi.v9i1.1921
**Copyright** © 2026 by the authors. Published by Jurusan Teknik Elektromedik, Politeknik Kesehatan Kemenkes Surabaya Indonesia. This work is an open-access article and licensed under a Creative Commons Attribution-ShareAlike 4.0 International License (CC BY-SA 4.0).

## Declarations

### Ethical Approval

Ethical approval was not required because this study involved exclusively laboratory-based mechanical testing of commercially available Solid Ankle Cushion Heel (SACH) prosthetic-foot components. No human participants, animals, human biological specimens, or identifiable personal data were involved.

### Consent to Participate

Not applicable. This study did not involve human participants or the collection of personal information.

### Consent for Publication

Not applicable to participant consent, as the study did not involve human participants or identifiable personal data. All authors have reviewed and approved the final manuscript and agreed to its submission for publication.

### Competing Interests

The authors declare that they have no financial or non-financial competing interests that could have influenced the research, analysis, interpretation, or reporting of the findings. The commercial SACH prosthetic feet were identified using anonymized internal inventory codes, and no endorsement of any manufacturer or commercial product is implied.

### Declaration of Generative Artificial Intelligence and AI-Assisted Technologies

During the preparation of this manuscript, the authors used Claude (Anthropic) to assist with language editing, improving readability and manuscript organization, and revising the manuscript in response to editorial comments. The AI-assisted tool was not used to generate, fabricate, or modify experimental measurements, laboratory observations, statistical results, or scientific conclusions.

All AI-assisted content was critically reviewed, verified, and edited by the authors. The authors take full responsibility for the accuracy, originality, integrity, and final content of the published manuscript. No AI-assisted tool is listed as an author.

### Research Integrity and Data Authenticity

The authors confirm that the experimental observations and results reported in this manuscript were derived from laboratory mechanical testing records. The reported loading deviations, differences in specimen exposure, and limitations of the visual microdeformation assessment have been disclosed transparently. No experimental values were intentionally fabricated, falsified, or selectively modified. All authors accept responsibility for the integrity and accuracy of the reported findings.

## References

[1] A. S. Nugroho, K. Sasaki, M. Nouman, and R. Ismail, “Design and Mechanical Evaluation of a Polymer Keel SACH Foot Using Finite Element Analysis and Experimental Validation,” J. Electron. Electromed. Eng. Med. Informatics, vol. 8, no. 3, pp. 1148–1162, Jul. 2026, doi: 10.35882/jeeemi.v8i3.1807.

[2] K. Alluhydan, M. I. H. Siddiqui, and H. Elkanani, “Functionality and Comfort Design of Lower-Limb Prosthetics: A Review,” J. Disabil. Res., vol. 2, no. 3, Sep. 2023, doi: 10.57197/JDR-2023-0031.

[3] T. M. Balaramakrishnan, S. Natarajan, and S. Sujatha, “Design of a Biomimetic SACH Foot: An Experimentally Verified Finite Element Approach,” J. Biomimetics, Biomater. Biomed. Eng., vol. 45, pp. 22–30, May 2020, doi: 10.4028/www.scientific.net/JBBBE.45.22.

[4] M. Falbriard et al., “A functional approach towards the design, development, and test of an affordable dynamic prosthetic foot,” PLoS One, vol. 17, no. 5, p. e0266656, May 2022, doi: 10.1371/journal.pone.0266656.

[5] B. J. Hafner, E. G. Halsne, S. J. Morgan, D. C. Morgenroth, and A. T. Humbert, “Effects of prosthetic feet on metabolic energy expenditure in people with transtibial amputation: A systematic review and meta-analysis,” PM&R, vol. 14, no. 9, pp. 1099–1115, Sep. 2022, doi: 10.1002/pmrj.12693.

[6] World Health Organization and UNICEF, Global report on assistive technology. Geneva, Switzerland: World Health Organization, 2022.

[7] F. M. Kadhim, S. A. Fadhil, A. M. Abdullah, and M. S. Al-Din Tahir, “Designing and manufacturing a flexible heel of a printed prosthetic foot for rehabilitation,” Int. Rev. Appl. Sci. Eng., vol. 16, no. 2, pp. 324–330, Jun. 2025, doi: 10.1556/1848.2024.00930.

[8] S. L. Sashenkov, A. N. Panasenko, A. A. Episheva, F. V. Merkulyev, Y. V. Burnashov, and A. A. Piskaev, “Analysis of Opportunities for the Development of a Brand-New Prosthetic Foot,” Hum. Sport Med., vol. 23, no. 4, pp. 155–162, 2023, doi: 10.14529/hsm230419.

[9] T. M. Balaramakrishnan, S. Natarajan, and S. Sujatha, “Biomechanical design framework for prosthetic feet: Experimentally validated non-linear finite element procedure,” Med. Eng. Phys., vol. 92, no. 1, pp. 64–70, Jun. 2021, doi: 10.1016/j.medengphy.2021.04.006.

[10] E. N. Abbas, K. K. Resan, M. J. Jweeg, E. K. Njim, and R. Madan, “Fabrication and experimental analysis of a novel flexible keel

Manuscript Received 16 September 2026; Accepted: 10 November 2026; Published online: 20 November 2026
**Digital Object Identifier (DOI):** https://doi.org/10.35882/jeeemi.v9i1.1921
**Copyright** © 2026 by the authors. Published by Jurusan Teknik Elektromedik, Politeknik Kesehatan Kemenkes Surabaya Indonesia. This work is an open-access article and licensed under a Creative Commons Attribution-ShareAlike 4.0 International License (CC BY-SA 4.0).

prosthetic foot utilizing functionally graded materials," J. Med. Eng. Technol., vol. 50, no. 1, pp. 56–64, Jan. 2026, doi: 10.1080/03091902.2025.2570158.

[11] H. A. Abdalwahhab and K. K. Resan, "Development and mechanical analysis of a novel prosthetic foot with a flexible keel for improved functionality," in The International Middle Eastern Simulation and Modelling Conference, MESM 2023, 2024, pp. 71–75.

[12] P. Chauhan, A. K. Singh, and N. K. Raghuwanshi, "The state of art review on prosthetic feet and its significance to imitate the biomechanics of human ankle-foot," Mater. Today Proc., vol. 62, pp. 6364–6370, 2022, doi: 10.1016/j.matpr.2022.03.379.

[13] N. Worajinda, J. Phromjan, R. Rugsaj, S. Phakdee, and C. Suvanjumrat, "Design and Analysis of a Composite SACH Foot: Experimental Validation and Finite Element Modeling," Key Eng. Mater., vol. 1016, pp. 115–120, Jun. 2025, doi: 10.4028/p-6LrQlL.

[14] P. Maroti et al., "Additive manufacturing in limb prosthetics and orthotics: the past, present and future of 3D printing orthopedic assistive devices," in Medical Additive Manufacturing, Elsevier, 2024, pp. 179–207. doi: 10.1016/B978-0-323-95383-2.00028-7.

[15] M. Omasta, D. Paloušek, T. Návrat, and J. Rosický, "Finite element analysis for the evaluation of the structural behaviour, of a prosthesis for trans-tibial amputees," Med. Eng. Phys., vol. 34, no. 1, pp. 38–45, Jan. 2012, doi: 10.1016/j.medengphy.2011.06.014.

[16] V. Plesec, J. Humar, P. Dobnik-Dubrovski, and G. Harih, "Numerical Analysis of a Transtibial Prosthesis Socket Using 3D-Printed Bio-Based PLA," Materials (Basel)., vol. 16, no. 5, p. 1985, Feb. 2023, doi: 10.3390/ma16051985.

[17] A. Vasanthanathan, S. M. Kennedy, K. Amudhan, K. Jairooban, S. Karthikeyan, and B. Vignesh, "Design, optimization, FEA and fabrication of lightweight CFRP prosthetic foot," Prog. Eng. Sci., vol. 3, no. 1, p. 100200, Mar. 2026, doi: 10.1016/j.pes.2025.100200.

[18] A. R. N. Al Thahabi, L. M. Martulli, A. Sorrentino, M. Lavorgna, E. Gruppioni, and A. Bernasconi, "Stiffness-driven design and optimization of a 3D-printed composite prosthetic foot: A beam finite Element-Based framework," Compos. Struct., vol. 337, p. 118053, Jun. 2024, doi: 10.1016/j.compstruct.2024.118053.

[19] L. Baldassari, M. Minuto, E. Gruppioni, and M. Frascio, "Design, Testing and Validation of a Cost Effective and Sustainable Bamboo Prosthetic Foot," Prosthesis, vol. 7, no. 5, p. 124, Oct. 2025, doi: 10.3390/prosthesis7050124.

[20] K. Shah and M. U. Rehman, "Finite Element Analysis of Custom Designed and Additive Manufactured Total Surface Bearing Prosthesis for Trans-Tibial Amputees," Appl. Sci., vol. 15, no. 3, p. 1284, Jan. 2025, doi: 10.3390/app15031284.

[21] N. N. Subhash et al., "Structural Performance Assessment of FUPRO Grace Foot," Trends Biomater. Artif. Organs, vol. 36, no. 2, pp. 94–101, 2022.

[22] E. G. Halsne, J. M. Czerniecki, J. B. Shofer, and D. C. Morgenroth, "The effect of prosthetic foot stiffness on foot-ankle biomechanics and relative foot stiffness perception in people with transtibial amputation," Clin. Biomech., vol. 80, p. 105141, Dec. 2020, doi: 10.1016/j.clinbiomech.2020.105141.

[23] U. Trinler, D. W. W. Heitzmann, S. Hitzeroth, M. Alimusaj, M. Rehg, and A. Hogan, "Biomechanical comparison of a 3D-printed prosthetic foot with conventional feet in people with transtibial amputation: A prospective cohort study," Prosthetics Orthot. Int., vol. 47, no. 1, pp. 94–100, Feb. 2023, doi: 10.1097/PXR.0000000000000180.

[24] International Organization for Standardization, ISO 10328:2016 ProstheticsStructural testing of lower-limb prosthesesRequirements and test methods. Geneva, Switzerland: ISO, 2016.

[25] H. A. Abdalwahhab, K. Resan, and E. Omaraa, "Comparing Maximum Lifespan of a New Flexible Keel versus Non-Articulated Prosthetic Feet," J. Eng. Sustain. Dev., vol. 29, no. 1, pp. 89–95, Jan. 2025, doi: 10.31272/jeasd.2193.

[26] T. Mannan Balaramakrishnan, S. Natarajan, and S. Sujatha, "Energy storage and stress–strain characteristics of a prosthetic foot: a priori design and analysis with experiments," Int. j. numer. method. biomed. eng., vol. 38, no. 4, Apr. 2022, doi: 10.1002/cnm.3579.

[27] G. Barrera et al., "The Effect of Surface Treatments on the Mechanical Properties of Low-Density Polyethylene/Natural Rubber Composites Reinforced with Sugarcane Bagasse Ash," J. Compos. Sci., vol. 9, no. 9, p. 489, Sep. 2025, doi: 10.3390/jcs9090489.

[28] N. B. Mohammed and Yassr Y. Kahtan, "Developmental study of a 3D prosthetic foot using finite element analysis," Int. J. Adv. Technol. Eng. Explor., vol. 11, no. 120, Nov. 2024, doi: 10.19101/IJATEE.2024.111100971.

[29] S. G. Nukala, I. Kong, A. B. Kakarla, V. I. Patel, and H. Abuel-Naga, "Simulation of Wood

Manuscript Received 16 September 2026; Accepted: 10 November 2026; Published online: 20 November 2026
**Digital Object Identifier (DOI):** https://doi.org/10.35882/jeeemi.v9i1.1921
**Copyright** © 2026 by the authors. Published by Jurusan Teknik Elektromedik, Politeknik Kesehatan Kemenkes Surabaya Indonesia. This work is an open-access article and licensed under a Creative Commons Attribution-ShareAlike 4.0 International License (CC BY-SA 4.0).

Polymer Composites with Finite Element Analysis," Polymers (Basel)., vol. 15, no. 9, p. 1977, Apr. 2023, doi: 10.3390/polym15091977.

[30] J. P. M. Tribst, "Digital Image Correlation and Finite Element Analysis of Bone Strain Generated by Implant-Retained Cantilever Fixed Prosthesis," Eur. J. Prosthodont. Restor. Dent., vol. 28, no. 1, pp. 10–17, Mar. 2020, doi: 10.1922/EJPRD_1941Tribst08.

[31] D. Trindade et al., "Material Performance Evaluation for Customized Orthoses: Compression, Flexural, and Tensile Tests Combined with Finite Element Analysis," Polymers (Basel)., vol. 16, no. 18, p. 2553, Sep. 2024, doi: 10.3390/polym16182553.

[32] E. Pelita, T. R. Hidayani, and A. Akbar, "Analysis physical properties of composites polymer from cocofiber and polypropylene plastic waste with maleic anhydrate as crosslinking agent," IOP Conf. Ser. Mater. Sci. Eng., vol. 223, p. 012060, Jul. 2017, doi: 10.1088/1757-899X/223/1/012060.

[33] L. Indrie, S. McNeil, M. M. Mutlu, S. Bota, D. C. Ilieș, and H. A. Karavana, "The Initial Development and Evaluation of Cross-Linked Casein Films for Sustainable Footwear," Coatings, vol. 13, no. 2, p. 217, Jan. 2023, doi: 10.3390/coatings13020217.

[34] R. B. Al-Tameemi, H. Mazaheri, M. Shaban, and J. S. Chiad, "Biomechanical Comparison of SACH, Single-Axis, and Multi-Axis Prosthetic Feet with Osseointegrated Implants Using Ground Reaction Force," Int. J. Adv. Sci. Eng. Inf. Technol., vol. 16, no. 2, pp. 353–358, 2026, doi: 10.18517/ijaseit.16.2.21775.

[35] S. Bhatt, D. Joshi, P. K. Rakesh, and A. K. Godiyal, "Advances in additive manufacturing processes and their use for the fabrication of lower limb prosthetic devices," Expert Rev. Med. Devices, vol. 20, no. 1, pp. 17–27, Jan. 2023, doi: 10.1080/17434440.2023.2169130.

[36] A. K. Faizin, N. Adyono, W. D. Lestari, A. A. Yusuf, and M. I. Ammarullah, "A novel prosthetic foot with a flexible rubber ankle for the Indonesian population: a finite element analysis," BMC Musculoskelet. Disord., vol. 26, no. 1, p. 1119, Dec. 2025, doi: 10.1186/s12891-025-09418-w.

[37] A. Kurakin, A. Sergeev, D. Korostovskaya, A. Kurenkova, and V. Serdyukov, "Development and Comprehensive Evaluation of 3D-Printed Prosthetic Feet: Modeling, Testing and a Pilot Gait Study," Prosthesis, vol. 8, no. 4, p. 40, Apr. 2026, doi: 10.3390/prosthesis8040040.

[38] W. D. L. Lestari, Y. Ariadi, and A. Putra, "Customized Prosthetic Feet via Topology Optimization and 3D Printing: A Critical Review," Adv. Mech. Mechatron. Syst., vol. 2, no. 1, pp. 33–49, Dec. 2025, doi: 10.53623/amms.v2i1.776.

[39] F. Tavangarian, N. K. Khairunajhan, M. S. M. Yusairi, L. H. I. Nasir, F. H. Mazlan, and A. Attaluri, "3D printed pylon for lower limb prosthetic device inspired by spicule architecture," Explor. BioMat-X, vol. 2, Sep. 2025, doi: 10.37349/ebmx.2025.101347.

[40] J. S. Jensen and H. B. Treichl, "Mechanical testing of prosthetic feet utilized in low-income countries according to ISO-10328 standard," Prosthet. Orthot. Int., vol. 31, no. 2, pp. 177–206, Jun. 2007, doi: 10.1080/03093640701210986.

[41] Z. D. Mason, J. Pearlman, R. A. Cooper, and J. Z. Laferrier, "Comparison of prosthetic feet prescribed to active individuals using ISO standards," Prosthet. Orthot. Int., vol. 35, no. 4, pp. 418–424, Dec. 2011, doi: 10.1177/0309364611421692.

[42] K. Sasaki et al., "The development and testing of a modified natural rubber CR solid ankle–cushion heel prosthetic foot for developing countries," J. Rehabil. Assist. Technol. Eng., vol. 4, p. 2055668317712978, Jun. 2017, doi: 10.1177/2055668317712978.

[43] Joint Committee for Guides in Metrology, JCGM 100:2008 Evaluation of measurement dataGuide to the expression of uncertainty in measurement. Sèvres, France: BIPM, 2008.

[44] R. C. Hibbeler, Mechanics of Materials, 10th ed. Hoboken, NJ, USA: Pearson, 2017.

[45] R. I. Stephens, A. Fatemi, R. R. Stephens, and H. O. Fuchs, Metal Fatigue in Engineering, 2nd ed. New York, NY, USA: Wiley, 2001.

[46] M. A. Miner, "Cumulative damage in fatigue," J. Appl. Mech., vol. 12, no. 3, pp. A159–A164, Sep. 1945, doi: 10.1115/1.4009458.

[47] E. L. Kaplan and P. Meier, "Nonparametric estimation from incomplete observations," J. Am. Stat. Assoc., vol. 53, no. 282, pp. 457–481, Jun. 1958, doi: 10.1080/01621459.1958.10501452.

[48] E. B. Wilson, "Probable inference, the law of succession, and statistical inference," J. Am. Stat. Assoc., vol. 22, no. 158, pp. 209–212, Jun. 1927, doi: 10.1080/01621459.1927.10502953.

[49] O. H. Basquin, "The exponential law of endurance tests," Proc. Am. Soc. Test. Mater., vol. 10, pp. 625–630, 1910.

Manuscript Received 16 September 2026; Accepted: 10 November 2026; Published online: 20 November 2026
**Digital Object Identifier (DOI):** https://doi.org/10.35882/jeeemi.v9i1.1921
**Copyright** © 2026 by the authors. Published by Jurusan Teknik Elektromedik, Politeknik Kesehatan Kemenkes Surabaya Indonesia. This work is an open-access article and licensed under a Creative Commons Attribution-ShareAlike 4.0 International License (CC BY-SA 4.0).

## Author Biography



**Mahfud Saifudin** is an Applied Bachelor student in Prosthetics and Orthotics at Poltekkes Kemenkes Surakarta, Indonesia. His academic and research interests focus on lower-limb prosthetics, prosthetic-foot components, mechanical durability testing, and quality assurance of prosthetic devices. His research activities include laboratory-based evaluation of prosthetic components, with particular attention to the cyclic mechanical response and structural integrity of Solid Ankle Cushion Heel (SACH) prosthetic feet. He is interested in applying standardized mechanical testing to support evidence-based component selection, product evaluation, and quality control in prosthetic services. His work aims to contribute to safer, reliable, and accessible prosthetic rehabilitation technologies.



**Nur Rachmat** earned his Bachelor of Science with Honours in Prosthetics and Orthotics from the University of Peshawar in 2010, a Master of Health degree from Sebelas Maret University in 2013, and a Doctoral degree in Health Promotion in 2020. He is an Associate Professor and currently serves as Head of the Department of Prosthetics and Orthotics at Poltekkes Kemenkes Surakarta, Indonesia. His research interests encompass prosthetics and orthotics, rehabilitation biomechanics, functional mobility, assistive technology, and disability-related health and participation. His current research focuses particularly on lower-limb prosthetic rehabilitation, functional outcome assessment, sustainable and composite materials for prosthetic applications, and the development and evaluation of innovative assistive devices. He has developed innovations including coconut-coir composite transtibial prosthetic sockets and a patented anti-decubitus seat-pad cushion. In addition to teaching and research, he is actively engaged in clinical, industrial, and community-based collaborations. His work aims to advance evidence-based, accessible, and function-oriented prosthetic and orthotic technologies that enhance mobility, independence, participation, and quality of life for people with disabilities.



**Sisybania** is a lecturer in the Department of Orthotics and Prosthetics at Poltekkes Kemenkes Surakarta. She was born in Padang, Indonesia, on December 8, 1995. In 2013, she moved to Surakarta to pursue her education in Orthotics and Prosthetics at Poltekkes Kemenkes Surakarta. She subsequently pursued a Master's degree in Public Health at Universitas Sebelas Maret, specializing in Health Policy and Health Services Management. Her academic background in Orthotics and Prosthetics, complemented by her expertise in public health, supports her academic and professional roles in education, research, and the development of healthcare services, particularly in the field of orthotics and prosthetics.

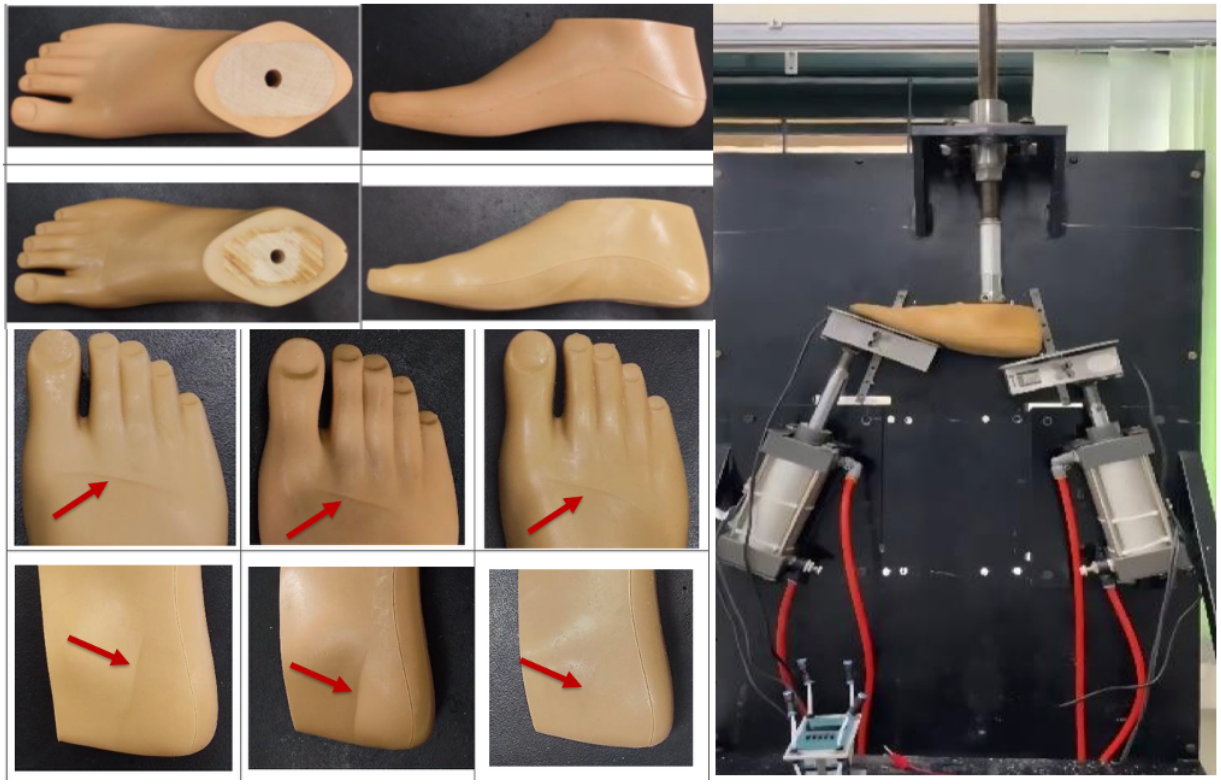


**Anissa Eka Septiani** is a lecturer in the Department of Orthotics and Prosthetics at Poltekkes Kemenkes Surakarta. She graduated with a Bachelor of Applied Orthotics and Prosthetics at Poltekkes Kemenkes Surakarta in 2017. She graduated with a Master's degree in Public Health at Universitas Sebelas Maret in 2021. Her academic and research interests focus on orthotics and prosthetics, particularly lower-limb orthoses, ankle-foot orthoses, foot orthoses, musculoskeletal rehabilitation, and functional outcomes of orthotic interventions. Her research has addressed the clinical application of ankle support, medial arch support, cervical orthoses, and ankle-foot orthoses for individuals with musculoskeletal and neurological conditions. She is actively involved in teaching, research, and community-based activities related to orthotic and prosthetic rehabilitation.

Manuscript Received 16 September 2026; Accepted: 10 November 2026; Published online: 20 November 2026
**Digital Object Identifier (DOI):** https://doi.org/10.35882/jeeemi.v9i1.1921
**Copyright** © 2026 by the authors. Published by Jurusan Teknik Elektromedik, Politeknik Kesehatan Kemenkes Surabaya Indonesia. This work is an open-access article and licensed under a Creative Commons Attribution-ShareAlike 4.0 International License (CC BY-SA 4.0).

Journal of Electronics, Electromedical Engineering, and Medical Informatics
Homepage: jeeemi.org; Vol. 9, No. 1, January 2027, pp: 54-76 e-ISSN: 2656-8632

# COVER IMAGE



Manuscript Received 16 September 2026; Accepted: 10 November 2026; Published online: 20 November 2026
**Digital Object Identifier (DOI):** https://doi.org/10.35882/jeeemi.v9i1.1921
**Copyright** © 2026 by the authors. Published by Jurusan Teknik Elektromedik, Politeknik Kesehatan Kemenkes Surabaya Indonesia. This work is an open-access article and licensed under a Creative Commons Attribution-ShareAlike 4.0 International License (CC BY-SA 4.0).